

Thermodynamics of the dissipative two-state system: a Bethe Ansatz study

T. A. Costi[†]

*Universität Karlsruhe, Institut für Theorie der Kondensierten Materie, 76128 Karlsruhe, Germany
Theoretische Physik III, Universität Augsburg, D-86135 Augsburg, Germany¹.*

G. Zaránd[‡]

*Research Group of the Hungarian Academy of Sciences, Institute of Physics, TU Budapest, P.O. Box 91, H-1521 Hungary
Physics Department, University of California, Davis, 1 Shields Avenue, 95616, U.S.A²*

The thermodynamics of the dissipative two-state system is calculated exactly for all temperatures and level asymmetries for the case of Ohmic dissipation. We exploit the equivalence of the two-state system to the anisotropic Kondo model and extract the thermodynamics of the former by solving the thermodynamic Bethe Ansatz equations of the latter. The universal scaling functions for the specific heat $C_\alpha(T)$ and static dielectric susceptibility $\chi_\alpha(T)$ are extracted for all dissipation strengths $0 < \alpha < 1$ for both symmetric and asymmetric two-state systems. The logarithmic corrections to these quantities at high temperatures are found in the Kondo limit $\alpha \rightarrow 1^-$, whereas for $\alpha < 1$ we find the expected power law temperature dependences with the powers being functions of the dissipative coupling α . The low temperature behaviour is always that of a Fermi liquid.

PACS numbers: 71.27.+a, 71.10.+x, 72.15.Qm

I. INTRODUCTION

The low temperature properties of many physical systems, such as quantum tunneling between flux states in a SQUID,¹ two-level atoms coupled to the electromagnetic field in quantum optics,² or tunneling dislocations and point defects in solids³ can be described by the dissipative two-state system model^{4,5}. All these systems have the common feature that at low energies the subsystem investigated (the flux states of the SQUID, the atom, or the crystal defect in the examples above) can occupy only two distinct quantum states, which are coupled to a continuum of excitations (the electromagnetic field, the phonons or the conduction electrons), leading to the appearance of dissipation in the system⁶.

In the dissipative two state system (DTSS) model the two distinct quantum states above are described in terms of a pseudospin σ_i , with $\sigma_z = \pm 1$ corresponding to the two states of the subsystem. Generally, these two states have slightly different energy with an energy difference ε (also called asymmetry energy) and the decoupled two-state system (TSS) can tunnel between them with a tunneling amplitude Δ . The heat bath is modeled by a continuum of independent quantum oscillators with density $\varrho(\omega)$ coupled linearly to σ_z with a frequency dependent coupling $g(\omega)$. A detailed analysis shows that the dynamical properties of the two-state system are uniquely determined by the environment's spectral function, $J(\omega) \sim \varrho(\omega)g^2(\omega) \sim \omega^{s5}$.

Here, we only concentrate on Ohmic dissipation corresponding to $s = 1$, i.e. $J(\omega) \sim \omega$. This includes, for instance, the important case of a tunneling defect in a metal, where the low-energy bosonic excitations are electron-hole pairs close to the Fermi surface. These exci-

tations have a linear dispersion, and in a first approximation their coupling to the defect is energy-independent, leading to $J(\omega) = 2\pi\alpha\omega$ for $\omega < \omega_c$ with ω_c a high-energy cutoff in the model of the order of the Fermi energy E_F . The dynamical behaviour of the TSS as a function of the coupling strength α has been the subject of extensive studies during the past two decades and it is well understood by now⁷. To distinguish between the different cases it is useful to introduce the zero temperature spin correlation function $S(t) \equiv \Im\langle\sigma_z(0)\sigma_z(t)\rangle$. (a) For $\alpha < 1/2$ the TSS oscillates between the two states $\sigma_z = \pm 1$ and $S(t)$ has an oscillatory behaviour. However, the environment introduces some decoherence in the system, reflected in the exponential decay of the envelope of $S(t)$. It also renormalizes the tunneling amplitude: $\Delta \rightarrow \Delta_r < \Delta$. (b) In the parameter range $1/2 < \alpha < 1$ the coherent oscillations⁸ become completely suppressed, and $S(t)$ shows an exponential behaviour without a change of sign. (c) Finally, for $\alpha > 1$ and a finite level asymmetry the TSS becomes localized in the lowest quantum state (at $T = 0$)¹⁰. In this case $S(t)$ tends to a *finite* value as $t \rightarrow \infty$. It is important to note that the localized state obtained is immediately destroyed once assisted tunneling or assisted pair tunneling is included in the DTSS model^{11,12}.

In the present paper we study the *thermodynamics* of a dissipative TSS model in the parameter range $0 < \alpha < 1$. To this purpose we exploit a mapping between the spin anisotropic Kondo model (AKM) describing an impurity spin coupled to the spin density of the conduction electrons via an anisotropic exchange interaction (see Sec. IIb) and the dissipative TSS model,^{4,5} and study the Bethe Ansatz equations¹³ for the former both numerically and analytically. As discussed in Sec. IIB and Appendix A, within this mapping the tunneling amplitude maps to the spin flip scattering amplitude, $\Delta \leftrightarrow J_\perp$, the asymmetry energy ε corresponds to a local magnetic field h applied to the impurity spin, and the dissipation

strength α is related to the coupling J_z in the Kondo model. It is very remarkable that the α values separating the three different regions of the DTSS model are mapped to some special points in the parameter space of the Kondo model. The point $\alpha = 1$ turns out to correspond to the case $J_z = 0$, separating the ferromagnetic ($J_z < 0 \Leftrightarrow \alpha > 1$) and the antiferromagnetic ($J_z > 0 \Leftrightarrow \alpha < 1$) regimes in the Kondo model. While in the first case the Kondo model scales to a finite fixed point, in the second the Kondo fixed point turns out to be at infinite coupling. The crossover to the 'strong coupling' regime happens at the so-called Kondo energy, T_K ,^{14,15} which can be identified with the renormalized tunneling amplitude in the DTSS model, $\Delta_r \sim T_K$. The other special point, $\alpha = 1/2$, can be shown to be equivalent to the Toulouse line¹⁶ of the AKM. Along this line the Bethe Ansatz (BA) equations simplify enormously, and the model can be described by a simple resonant level model without interaction.

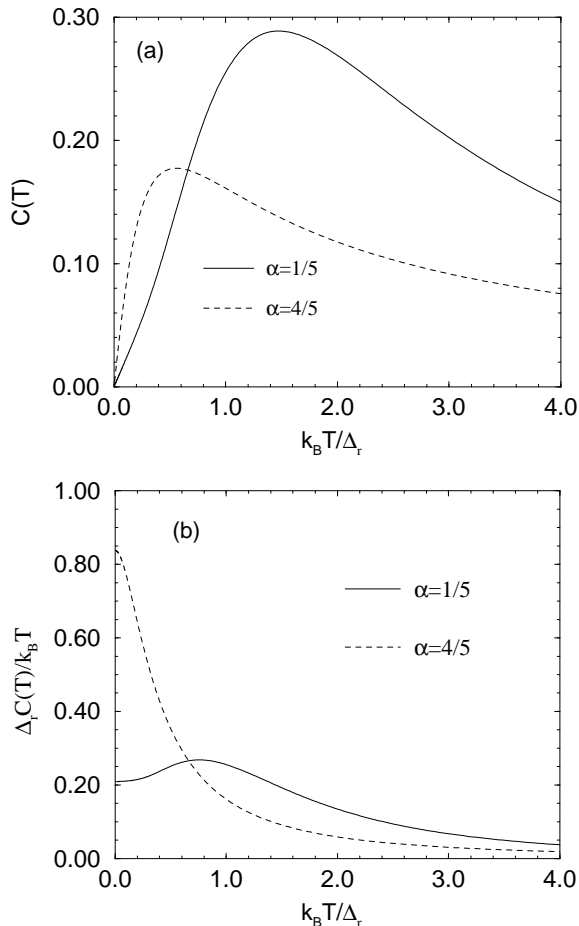


FIG. 1. (a) The specific heat $C(T)$ on a linear temperature scale for the symmetric case at weak and strong dissipations. The position of the maximum of the Schottky peak in $C(T)$ is of order Δ_r but its exact location changes with α , as does the peak height. (b) The quantity $\Delta_r C(T) / k_B T$ shows non-monotonic behaviour for weak dissipations, and monotonic behaviour for $\alpha \geq 1/3$.

We give a detailed description of the thermodynamics of the DTSS model, solving the BA equations for arbitrary asymmetry and temperature for both $\alpha > 1/2$ and $\alpha < 1/2$. For the sake of completeness and clarity, we also included a detailed analysis of the two models to demonstrate, how the different concepts such as scaling, strong coupling limit, energy scales, etc. appear in the AKM and the DTSS model. As we shall see, there are clear indicators in the specific heat, $C(T)$, for distinguishing weak from strong dissipation limits. This is not evident in $C(T)$ directly, which shows a Schottky anomaly at $k_B T \sim \Delta_r$ for all dissipation strengths $\alpha < 1$ as depicted in Fig. 1a. However, as seen in Fig. 1b, and as we shall discuss in detail later, the quantity $C(T)/T$, shows quite different behaviour at weak and strong dissipations. For dissipations $\alpha < 1/3$, with no asymmetry, $C(T)/T$ is found to have a peak at $k_B T \sim \Delta_r$ indicating the expected tendency towards activated behaviour of the two-level system as $\alpha \rightarrow 0$. A quite different behaviour is found for $\alpha \geq 1/3$ where we find that $C(T)/T$ is monotonically decreasing with increasing temperature. The tendency towards activated behaviour, signaled by a peak at approximately $\sqrt{\Delta_r^2 + \varepsilon^2}$ in $C(T)/T$, is also found at all dissipation strengths for sufficiently large (typically of order Δ_r) asymmetries ε . In the Kondo language this corresponds to the Zeeman splitting of the Kondo resonance due to a local magnetic field. In contrast, the dielectric susceptibility, $\chi_{sb} = -\partial^2 F / \partial \varepsilon^2$, with $F(T)$ the two-level system free energy, shows only a monotonically decreasing behaviour with increasing temperature for all dissipation strengths $0 < \alpha < 1$ in the symmetric case (see Fig. 2 and for further details Sec. IV C).

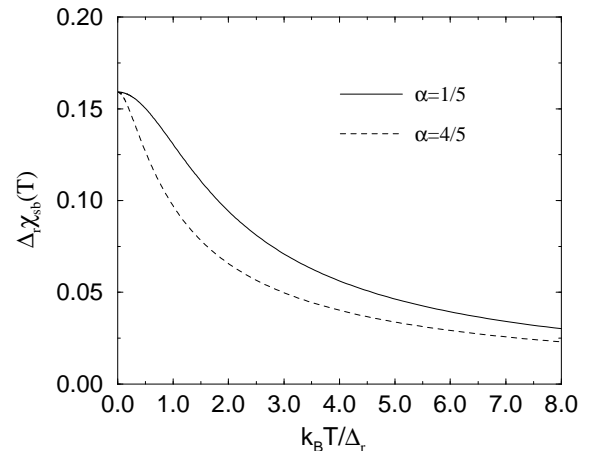


FIG. 2. The dielectric susceptibility, χ_{sb} , on a linear temperature scale for the symmetric case at weak and strong dissipations.

A peak in $\chi_{sb}(T)$ at finite temperature only appears for a sufficiently large level asymmetry. The low temperature behaviour corresponds to that of a renormalized Fermi liquid at all $\alpha < 1$ with the renormalizations increasing with α . Beyond these overall features we also discuss

the detailed form of the universal scaling functions of the dissipative two-state system for all $\alpha < 1$ and ε .

The only previous detailed studies of the thermodynamics of the Ohmic two-state system which we are aware of are, (a), the numerical renormalization group study¹⁷ and, (b), the work of Görlich and Weiss¹⁸. The latter authors used a path integral method⁴ to calculate the partition function of the dissipative two-state system for both Ohmic and non-Ohmic dissipation. Their results are restricted to weak level asymmetries $\varepsilon \ll \Delta_r$ and no results are presented for the finite temperature dielectric susceptibility. For the Ohmic case and $\alpha \ll 1$ they recover the linear T behaviour of the specific heat at low temperature $k_B T \ll \Delta_r$ and the correct high temperature behaviour at all α , however reliable results for strong dissipation $1/2 < \alpha < 1$ could not be obtained within their perturbative approach. The numerical renormalization group calculations in¹⁷ are non-perturbative and gave the specific heat accurately for all temperatures at both weak and strong dissipations. A drawback of this method, however, is the logarithmic discretization^{27,28} of the fermionic environment. This limits the ability of the method to resolve finite temperature features, such as the peak in $C(T)/T$ at $k_B T \sim \Delta_r$ for $\alpha \ll 1$. The calculation of the dielectric susceptibility by this method¹⁷ is also problematical at sufficiently low temperatures $k_B T \leq \Delta_r$ ¹⁹. As explained in¹⁷, accurate results for χ_{sb} at $T = 0$ required an analysis of the strong-coupling fixed point Hamiltonian together with the leading irrelevant deviations. Thus, this method gave accurate results for χ_{sb} at $T = 0$ (from the fixed point analysis) and for $k_B T \geq \Delta_r$, but it was not possible within this method to determine equally accurately the behaviour of χ_{sb} for $0 < k_B T \leq \Delta_r$. As we shall see the Bethe Ansatz method we use in this paper overcomes all the above difficulties.

The paper is organized as follows: in Sec. II we introduce the model of the dissipative two-state system and outline its equivalence to the anisotropic Kondo model for the case of Ohmic dissipation. Some implications of the Anderson-Yuval scaling picture of the anisotropic Kondo model for the Ohmic two-state system are briefly discussed. This gives a qualitative understanding of the physics of the latter in both the tunneling and localized regimes in terms of the fixed points, their stability and their associated low energy scales. Finally we show the connection between the scaling picture and the renormalization group flow obtained from the exact solution of the AKM via the Bethe Ansatz. The correspondence between the models via bosonization, described in Appendix A, is then used to translate the thermodynamic Bethe Ansatz equations for the anisotropic Kondo model, derived by Tselik and Wiegman, into the language of the Ohmic two-state system in Sec. III for both strong dissipation, $\alpha > 1/2$, (or weak anisotropy in the Kondo model) and weak dissipation, $\alpha < 1/2$ (or large anisotropy in the Kondo model) and at any level asymmetry ε (or local magnetic field in the Kondo model). Analytic results are then presented for the specific heat

and dielectric susceptibility of the two-state system at high and low temperatures and arbitrary dissipation in Sec. III B 2 and at all temperatures at the Toulouse point ($\alpha = 1/2$) in Sec. III B 4. The Wilson ratio for the Ohmic two-state system is discussed in Sec. III B 3. Sec. IV gives the numerical solution of the thermodynamic Bethe Ansatz equations at all temperatures for both weak and strong dissipation and for both symmetric and asymmetric two-level systems. Our conclusions are summarized in Sec. V. Appendix B contains some details on the Bethe Ansatz solution of the AKM and the corresponding thermodynamic Bethe Ansatz (TBA) equations which we solved in this paper. Appendix C gives details of the numerical procedure used to solve the TBA equations and Appendix D contains the universal TBA equations for weak dissipation (large anisotropies in the AKM), with some corrections made to those found originally in Ref. 13

II. MODELS

A. The dissipative two-state system

The model of the dissipative two-state system is given by

$$H_{SB} = -\frac{1}{2}\hbar\Delta\sigma_x + \frac{1}{2}\varepsilon\sigma_z + \sum_i \omega_i (a_i^\dagger a_i + \frac{1}{2}) + \frac{1}{2}q_0\sigma_z \sum_i \frac{C_i}{\sqrt{2m_i\omega_i}}(a_i + a_i^\dagger). \quad (1)$$

Here σ_i , $i = x, y, z$ are Pauli spin matrices, the two states of the system correspond to $\sigma_z = \uparrow$ and $\sigma_z = \downarrow$. Δ is the bare tunneling matrix element and ε is a bias. The environment is represented by an infinite set of harmonic oscillators (labeled by the index i) with masses m_i and frequency spectrum ω_i coupling linearly to the coordinate $Q = \frac{1}{2}q_0\sigma_z$ of the two-level system via a term characterized by the couplings C_i . The environment spectral function is given in terms of these couplings, oscillator masses and frequencies by $J(\omega) = \frac{\pi}{2} \sum_i (\frac{C_i^2}{m_i\omega_i}) \delta(\omega - \omega_i)$. In the case of an Ohmic heat bath, of interest to us here, we have $J(\omega) = 2\pi\alpha\omega$, for $\omega \ll \omega_c$, where ω_c is a high energy cut-off and α is a dimensionless parameter characterizing the strength of the dissipation. The Ohmic two-state model (also called the Ohmic spin-boson model) has been intensively studied (for reviews we refer the reader to^{4,5}). The model has a low energy scale, $\Delta_r < \Delta$ for $\Delta \ll \omega_c$, which depends on the dissipation strength α , and which may be interpreted as a renormalized tunneling *amplitude*. For $\alpha = 0$ the two-level system is decoupled from the environment and $\Delta_r = \Delta$, whereas with increasing coupling to the environment, this energy scale is strongly renormalized: $\Delta_r/\omega_c \sim (\Delta/\omega_c)^{1/(1-\alpha)}$. Another scale, the frequency of tunneling oscillations, $\Omega(\alpha, \Delta_r) = Q(\alpha)\Gamma(\alpha, \Delta_r)$, is relevant for time dependent quantities. Here $\Gamma(\alpha, \Delta_r) \sim \Delta_r$

is the decay rate and $Q(\alpha) = \cot(\frac{\pi}{2} \frac{\alpha}{1-\alpha})$ is the quality factor of the oscillations⁴. The latter vanishes at the Toulouse point $\alpha = \frac{1}{2}$, where the tunneling oscillations vanish (the “coherence-decoherence” crossover). For $0 < \alpha < 1/2$ the dynamics corresponds to damped oscillations of frequency $\Omega(\alpha, \Delta_r)$ ^{4,5,26}. This is sometimes called the “coherent”⁸ regime. The system exhibits phase coherence through this regime, albeit with damped oscillatory contributions to real time dynamical quantities. A smooth crossover to “incoherent” behaviour occurs at $\alpha = 1/2$. The tunneling amplitude remains finite in the “incoherent” regime $1/2 \leq \alpha < 1$, but there is no phase coherence in time dependent dynamical quantities: $\Omega(\alpha, \Delta_r) = 0$ for $\alpha \geq 1/2$. Another physically relevant value of the dissipation strength is $\alpha = 1/3$, where an inelastic peak, present in the neutron scattering cross-section for $\alpha < 1/3$, vanishes and gives rise to a quasielastic peak for $\alpha > 1/3$ ^{23–25} (see also the discussion in Sec. IV B 1). Finally, for sufficiently strong dissipation $\alpha \rightarrow 1^-$, the renormalized tunneling amplitude vanishes giving rise to the phenomenon of “localization” or “self-trapping” for $\alpha > \alpha_c \approx 1$ (α_c depends also on the precise value of Δ). In this paper we will be interested only in the thermodynamics of the dissipative two-state system. For such quantities the exact solution shows that, in the tunneling regime ($0 < \alpha < 1$)²⁰, the only relevant scale is Δ_r .

B. Equivalence to the anisotropic Kondo model

The equivalence of the Ohmic two-state system to the anisotropic Kondo model (AKM) has been shown at the Hamiltonian level via bosonization²¹ as outlined in Appendix A. This equivalence was believed to be valid in the region $\alpha > 1/2$, which corresponds (see below for the precise statement of the equivalence) to the region in the parameter space of the AKM between weak-coupling ($\rho J_{\parallel} \ll 1$) and the Toulouse point ($\rho J_{\parallel} \approx 1$). Recent work²³ shows that the equivalence extends beyond the Toulouse point into the region describing weak dissipation $0 < \alpha < 1/2$ (or large antiferromagnetic J_{\parallel} in the AKM, see also²⁹). The AKM is given by³⁰

$$H = \sum_{k,\sigma} \varepsilon_k c_{k\sigma}^\dagger c_{k\sigma} + \frac{J_{\perp}}{2} \sum_{kk'} (c_{k\uparrow}^\dagger c_{k'\downarrow} S^- + c_{k\downarrow}^\dagger c_{k'\uparrow} S^+) + \frac{J_{\parallel}}{2} \sum_{kk'} (c_{k\uparrow}^\dagger c_{k'\uparrow} - c_{k\downarrow}^\dagger c_{k'\downarrow}) S^z + g\mu_B h S_z. \quad (2)$$

The first term represents non-interacting conduction electrons and the second and third terms represent an exchange interaction between a localized spin 1/2 and the conduction electrons with strength J_{\perp}, J_{\parallel} . The last term in Eq. (2) is a local magnetic field, h , coupling only to the impurity spin. The correspondence between H and H_{SB} , outlined in Appendix A, requires that

$$\varepsilon = g\mu_B h \quad (3)$$

$$\frac{\Delta}{\omega_c} = \rho J_{\perp} \quad (4)$$

$$\alpha = (1 + \frac{2\delta}{\pi})^2, \quad (5)$$

where $\tan \delta = -\frac{\pi \rho J_{\parallel}}{4}$, δ is the phase shift for scattering of electrons from a potential $J_{\parallel}/4$ and $\rho = 1/2D$ is the conduction electron density of states per spin at the Fermi level for a flat band of width $2D = \omega_c$ ^{4,23}. We note that weak dissipation ($\alpha \rightarrow 0$) in the Ohmic two-state model corresponds to large antiferromagnetic coupling ($J_{\parallel} \rightarrow \infty$) in the Kondo model whereas dissipation strength $\alpha > 1$ in the Ohmic two-state model corresponds to ferromagnetic coupling $J_{\parallel} < 0$ in the Kondo model.

C. Renormalization group flow

The renormalization group flow of the Ohmic two-state system can be obtained by making use of the above equivalence and the Anderson-Yuval scaling equations³⁰ for the AKM. These equations hold to lowest order in ρJ_{\perp} but for all ρJ_{\parallel} : $-\infty < \rho J_{\parallel} < +\infty$. They are therefore valid for all $0 \leq \alpha \leq 4$ provided $\Delta/\omega_c \ll 1$. The Anderson-Yuval scaling equations extend the validity of the well known Poor Man’s scaling equations to the whole J_{\parallel} axis and reduce to those when $\rho J_{\parallel} \ll 1$. In terms of the dimensionless quantities ρJ_{\perp} and

$$\tilde{\varepsilon} = -8 \frac{\delta}{\pi} (1 + \frac{\delta}{\pi}) \quad (6)$$

where δ was defined above, the Anderson-Yuval scaling equations read^{30,4}

$$\begin{aligned} \frac{d\tilde{\varepsilon}}{d \ln D} &= (\tilde{\varepsilon} - 2)(\rho J_{\perp})^2 + \mathcal{O}(\rho J_{\perp})^4 \\ \frac{d\rho J_{\perp}}{d \ln D} &= -\frac{\tilde{\varepsilon}}{2} \rho J_{\perp} + \mathcal{O}(\rho J_{\perp})^3 \end{aligned} \quad (7)$$

By using the correspondence between the models given above, and noting that $\tilde{\varepsilon} = 2(1 - \alpha)$, we obtain the following scaling equations for the Ohmic two-state system

$$\frac{d\alpha}{d \ln \omega_c} = \alpha \left(\frac{\Delta}{\omega_c}\right)^2 + \mathcal{O}\left(\frac{\Delta}{\omega_c}\right)^4 \quad (8)$$

$$\frac{d(\Delta/\omega_c)}{d \ln \omega_c} = -(1 - \alpha) \left(\frac{\Delta}{\omega_c}\right) + \mathcal{O}\left(\frac{\Delta}{\omega_c}\right)^3 \quad (9)$$

Note that in these equations α and Δ are running variables which are functions of the running cut-off, ω_c . The equations have to be supplemented by specifying initial conditions

$$\begin{aligned} \alpha(\omega_c = \omega_0) &= \alpha_0 \\ \Delta(\omega_c = \omega_0) &= \Delta_0. \end{aligned}$$

where $\alpha_0, \Delta_0, \omega_0$ are now the parameters appearing in the bare Hamiltonian (where they appeared as α, Δ, ω_c). We shall use this notation for the remainder of this section.

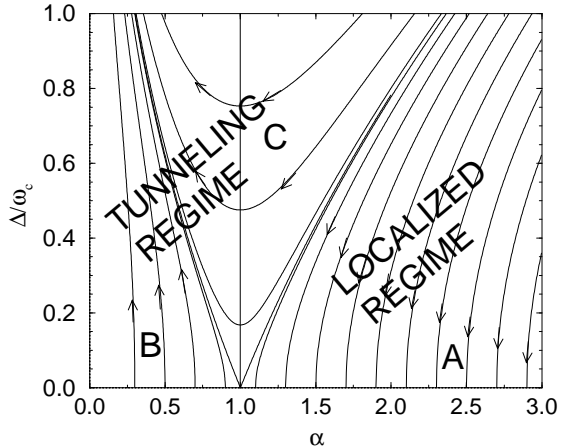


FIG. 3. The scaling trajectories of the Ohmic two-state system obtained from the Anderson-Yuval scaling equations for the AKM. Only the region $0 < \alpha < 3$ is shown. The left and right separatrices at $\alpha = 1, \Delta/\omega_c = 0$ define the regions labeled A, B and C and the arrows indicate the direction of decreasing ω_c .

From (8–9) there is a line of fixed points at $\Delta_0/\omega_0 = 0$ for $\alpha_0 \geq 0$. Their stability to a finite Δ_0/ω_0 follows from (9), which states that Δ/ω_c is relevant, marginal or irrelevant depending on whether the dissipation strength α_0 is less than, equal to or larger than 1³¹. Hence, the line of fixed points at $\Delta_0/\omega_0 = 0$ for $\alpha_0 > 1$ are stable low energy fixed points, whereas the line of fixed points at $\Delta_0/\omega_0 = 0$ for $\alpha_0 \leq 1$ are unstable high energy fixed points. The scaling trajectories can be calculated by dividing the two equations (8–9) and integrating the resulting equation from ω_0 down to ω_c :

$$\frac{1}{2} \left[\left(\frac{\Delta}{\omega_c} \right)^2 - \left(\frac{\Delta_0}{\omega_0} \right)^2 \right] = -((\ln \alpha - \alpha) - (\ln \alpha_0 - \alpha_0)) \quad (10)$$

They are shown in Fig.(3). The arrows indicate the direction of decreasing ω_c . When the flow is to strong coupling, the scaling trajectories will be quantitatively correct only for $\Delta/\omega_c \ll 1$. The scaling diagram is divided into three regions by two separatrices meeting at $\alpha = 1, \Delta/\omega_c = 0$.

The regime A ($\alpha_0 > 1$) corresponds to the localized regime of the Ohmic two-state system (or the ferromagnetic sector of the AKM). The dimensionless tunneling amplitude Δ/ω_c is irrelevant and the flow is to a line of fixed points ($\alpha = \alpha^*$ and $\Delta/\omega_c = 0$). This case is easily analyzed since the scaling equations remain valid as $\omega_c \rightarrow 0$. Since Δ/ω_c decreases as $\omega_c \rightarrow 0$, it follows from (8) that α remains almost unrenormalized: $\alpha \rightarrow \alpha^* \approx \alpha_0$ as $\omega_c \rightarrow 0$. Integrating (9) gives a renormalized tunneling amplitude $\Delta_r \equiv \Delta(\omega_c) = \Delta_0(\omega_c/\omega_0)^{\alpha_0}$ which vanishes at $T = 0$ at low energies. Quantum mechanical tunneling

is absent for $\alpha_0 > 1$ at $T = 0$ and for sufficiently small Δ_0/ω_0 .

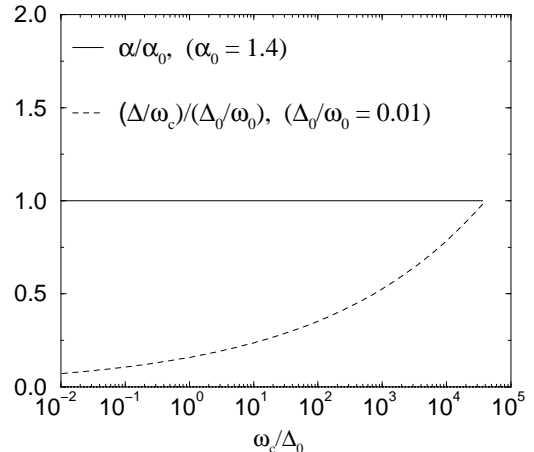


FIG. 4. Flow of running coupling constants in the localized region A of Fig. 3, for $\alpha_0 = 1.4$ and $\Delta_0/\omega_0 = 0.01$.

At finite temperature the low energy cut-off ω_c is replaced by $k_B T$ resulting in the well known temperature dependent tunneling amplitude $\Delta_r(T) = \Delta_0(k_B T/\omega_0)^{\alpha_0}$ in the strong dissipation limit. Fig. 4 shows the flow of the dimensionless coupling constants for a typical case in the localized regime. These were obtained by integrating (8–9) using the Runge-Kutta algorithm for 1st order differential equations.

The regime B ($\alpha < 1$) corresponds to the tunneling regime of the Ohmic two-state system (or the antiferromagnetic sector of the AKM): in this regime Δ/ω_c is relevant and the flow for $0 < \alpha_0 \leq 1$ is away from the line of high energy fixed points at $\Delta/\omega_c = 0$ towards the strong coupling fixed point at $\alpha = 0$ and $\Delta/\omega_c = \infty$. This is shown in the numerical solution of (8–9), in Fig. 5a. The scaling analysis, of course, breaks down when $\Delta/\omega_c = O(1)$, however, other methods, such as the numerical renormalization group and the Bethe Ansatz, show that the low energy fixed point is at $\Delta/\omega_c = \infty$ and $\alpha = 0$. In this regime, $\Delta(\omega_c)$ tends to a finite renormalized tunneling amplitude, Δ_r as $\omega_c \rightarrow 0$. In the AKM this low energy scale is the Kondo scale, generalized to the anisotropic case. We can estimate the $T = 0$ renormalized tunneling amplitude as the crossover scale separating weak ($\Delta/\omega_c \ll 1$) and strong coupling ($\Delta/\omega_c \gg 1$) regimes of the model. Define $\Delta_r = \Delta(\tilde{\omega}_c)$ where $\tilde{\omega}_c$ is the crossover scale such that $\Delta(\tilde{\omega}_c)/\tilde{\omega}_c = 1$. Integrating (9) down to this crossover scale

$$\int_1^{\frac{\Delta_0}{\omega_0}} \frac{d(\Delta/\omega_c)}{\Delta/\omega_c} = - \int_{\tilde{\omega}_c}^{\omega_0} (1 - \alpha) d \ln \omega_c \quad (11)$$

and approximating α by α_0 over this energy range gives

$$\Delta_r/\omega_0 = (\Delta_0/\omega_0)^{\frac{1}{1-\alpha_0}}, \quad (12)$$

the correct low energy scale for the Ohmic two-state system, up to prefactors depending on α_0 .

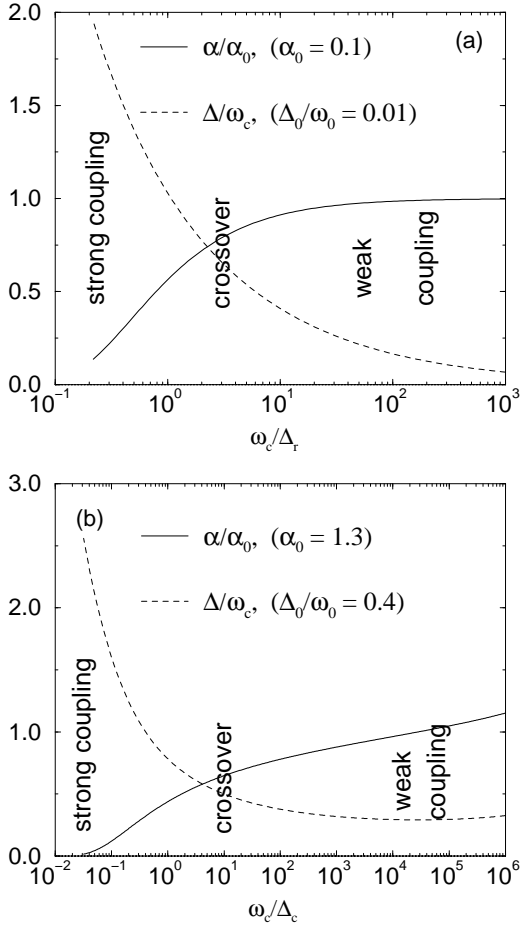


FIG. 5. Flow of running coupling constants for (a) $\alpha_0 = 0.1$ and $\Delta_0/\omega_0 = 0.01$ corresponding to the tunneling region B in Fig. 3, and (b) $\alpha_0 = 1.3$ and $\Delta_0/\omega_0 = 0.4$ corresponding to the tunneling region C in Fig. 3. In (b), Δ_c is a crossover scale at which Δ becomes of $O(1)$.

Finally, there is a region C, of strong dissipation, which also corresponds to the tunneling regime of the Ohmic two-state system. However, the flow to the strong coupling fixed point is such that, for $\alpha_0 > 1$, Δ/ω_c initially decreases with decreasing ω_c , signaling a tendency to localization for strong dissipation, but eventually, as a result of a strong renormalization of α to below 1, Δ/ω_c becomes relevant and then increases to strong coupling. The flow is to the same strong coupling fixed point as for region B and therefore region C belongs to the tunneling regime of the model. Due to the strong renormalization of α , Fig. 5b, it is difficult to estimate the form of the low energy scale Δ_r in this case.

The renormalization group flow described above consists of a one parameter family of scaling trajectories labeled by a parameter $C = C(\alpha, \Delta)$ which takes a constant value along each trajectory. This constant of the motion is called a scaling invariant and can be found from (10):

$$C(\alpha, \Delta) = -1 - \frac{1}{2} \left(\frac{\Delta}{\omega_c} \right)^2 - (\ln \alpha - \alpha) \quad (13)$$

Corresponding to this one parameter family of scaling trajectories we expect the scaling functions for physical quantities to consist of a one parameter family labeled by C , with different scaling functions for each scaling trajectory. The scaling invariant C is not unique but depends on the cut-off scheme of the theory. A scaling trajectory may be specified differently (i.e. by a different function C) depending on the cut-off scheme. One then has to identify the scaling trajectories within the different schemes if one wishes to compare results. The Bethe Ansatz solution of the AKM, which we want to use in the next section, is an example where such a different scheme is used. We state here how we identify the scaling trajectories of the Bethe Ansatz solution with those we discussed above for the Ohmic two-state system (or equivalently the AKM with a finite bandwidth $2D = \omega_c$) and leave the details to Appendix B. As discussed in the appendix, the Bethe Ansatz solution yields a renormalization group flow depending on two functions, μ and f , of the dimensionless couplings of the AKM. The function μ is the scaling invariant and specifies the scaling trajectories and the function f sets the low energy scale

$$T_K = 2D \exp(-f/(\mu/\pi)). \quad (14)$$

Comparing the high-temperature behaviour of the two models we find the correspondence

$$\mu/\pi = 1 - \alpha_0. \quad (15)$$

We shall show in Sec. III B 3 that the static susceptibility, χ_{BA} , calculated from the Bethe Ansatz solution is equal to the dielectric susceptibility, χ_{sb} , of the Ohmic two-state system and that, at $T = 0$, these are related to the Kondo temperature, as defined above, by

$$\chi_{BA} = \chi_{sb} = \frac{1}{2\pi(1 - \mu/\pi)T_K} = \frac{1}{2\pi\alpha_0 T_K}. \quad (16)$$

This suggests that we define the renormalized tunneling amplitude Δ_r in terms of T_K by³²

$$\Delta_r = \alpha_0 T_K \quad (17)$$

so that the local $T = 0$ dielectric susceptibility, χ_{sb} , of the Ohmic two-state system is given in terms of Δ_r by:

$$\chi_{sb} = \frac{1}{2\pi\Delta_r}. \quad (18)$$

The above relations fix f in terms of μ and T_K (or equivalently in terms of α_0 and Δ_r) and will prove useful in translating the Bethe Ansatz results of Sec III into results for the Ohmic two-state system.

III. THERMODYNAMIC BETHE ANSATZ EQUATIONS

A. Thermodynamic Bethe Ansatz equations for

$$\alpha = 1/\nu \text{ and } \alpha = 1 - 1/\nu$$

The thermodynamic Bethe Ansatz equations for the anisotropic Kondo model have been derived by Tsvetik and Wiegman¹³ (for a short overview of the derivation see Appendix B). For a general anisotropy they consist of an infinite set, $n = 1, 2, \dots$, of coupled integral equations for the “excitation energies” $\epsilon_n(\lambda)$ (defined in Appendix B). The thermodynamics is calculated from the impurity free energy which depends explicitly only on ϵ_1 . As discussed in¹³, the infinite set of integral equations for the ϵ_n decouple to a finite set for values of the anisotropy corresponding to rational values of the scaling invariant μ/π of the anisotropic Kondo model, and hence to rational values of the dissipation strength $\alpha = 1 - \mu/\pi$ in the Ohmic two-state system. In particular for anisotropies given by $\mu/\pi = 1/\nu$ and $\mu/\pi = 1 - 1/\nu$ with $\nu = 3, 4, \dots$, there are only ν coupled integral equations for the ν quantities $\epsilon_1, \epsilon_2, \dots, \epsilon_\nu$. These two cases allow us to study both the weak dissipation ($\alpha = 1/\nu < 1/2$) and the strong dissipation ($\alpha = 1 - 1/\nu > 1/2$) limits of the Ohmic two-state system. Explicitly, the ν coupled integral equations in Eq.6.2.11 of¹³ are

$$\begin{aligned} \frac{\epsilon_j(\lambda)}{T} &= s * \left[\ln\left(1 + \exp \frac{\epsilon_{j-1}}{T}\right) \left(1 + \exp \frac{\epsilon_{j+1}}{T}\right) \right. \\ &\quad \left. + \delta_{j,\nu-2} \ln\left(1 + \exp -\frac{\epsilon_\nu}{T}\right) \right] + \delta_{j,1} D(\lambda) \\ \frac{\epsilon_{\nu-1}(\lambda)}{T} &= x_0 + s * \ln\left(1 + \exp \frac{\epsilon_{\nu-2}}{T}\right), \\ \frac{\epsilon_\nu(\lambda)}{T} &= x_0 - s * \ln\left(1 + \exp \frac{\epsilon_{\nu-2}}{T}\right). \end{aligned} \quad (19)$$

Here $x_0 = \frac{1}{2} \frac{g\nu\varepsilon}{T}$, ε is the bias, $g = 1$ is a g -factor in the Kondo problem and $D(\lambda)$ is the driving term which is given explicitly by

$$D(\lambda) = -\text{sign}\left[\alpha - \frac{1}{2}\right] \frac{\omega_c}{T} \arctan(\exp(\pi\lambda)). \quad (20)$$

with ω_c a high energy cut-off (corresponding to the band width cutoff, D , in the Kondo model). The integral operator $s*$ is defined as in¹³:

$$s * f(\lambda) = \int_{-\infty}^{+\infty} \frac{1}{2 \cosh(\pi(\lambda - \lambda'))} f(\lambda') d\lambda'. \quad (21)$$

The ϵ_j 's ($j = 1, \dots, \nu$) satisfy boundary conditions at $\lambda = \pm\infty$ that can be obtained easily from Eq. (19). The impurity contribution to the free energy can be simply expressed as

$$F = -T \int_{-\infty}^{+\infty} s\left(\lambda + \frac{f}{\mu}\right) \ln\left(1 + e^{\epsilon_1(\lambda)/T}\right) d\lambda. \quad (22)$$

Eqs. (19) and (22) describe the complete thermodynamics of the model. Note that the field term x_0 in Eq. (19) represents a *global* magnetic field in the AKM coupling to

both the impurity and conduction electrons. However, as we discuss in Sec. III B 3, due to electron-electron interactions introduced to assure integrability, the impurity susceptibility of the BA solution, $-\partial^2 F/\partial\varepsilon^2$, coincides with the susceptibility of the Ohmic two-state system (i.e. with the impurity susceptibility of the AKM with a field coupling *only* to the impurity). Therefore the dielectric susceptibility, $\chi_{sb}(T, \varepsilon)$, and specific heat, $C(T, \varepsilon)$, of the Ohmic two-state system can be simply calculated as:

$$\chi_{sb}(T, \varepsilon) = -\partial^2 F/\partial\varepsilon^2, \quad (23)$$

$$C(T, \varepsilon) = -T\partial^2 F/\partial T^2. \quad (24)$$

B. Analytic results

1. Scaling and universality

A careful analysis of Eqs. (19) and (22) makes immediately transparent the meaning of universality. For $\mu < \pi/2$ ($\alpha > 1/2$) the impurity free energy can be shown to be dominated by contributions from the region $\lambda \ll 0$. In this limit the driving term can be approximated as $D(\lambda) \approx -\frac{\omega_c}{T} e^{\pi\lambda}$ and the explicit cutoff dependence can be transformed out of the equations by a simple shift, $\lambda \rightarrow \lambda + \frac{1}{\pi} \ln \frac{T}{\omega_c}$. In this way one arrives at the following universal equations for the quantities $\varphi_j(\lambda) \equiv \epsilon_j(\lambda + \frac{1}{\pi} \ln \frac{T}{\omega_c})/T$:

$$\begin{aligned} \varphi_j(\lambda) &= s * \left[\ln\left(1 + e^{\varphi_{j-1}}\right) \left(1 + e^{\varphi_{j+1}}\right) \right. \\ &\quad \left. + \delta_{j,\nu-2} \ln\left(1 + e^{-\varphi_\nu}\right) \right] - \delta_{j,1} e^{\pi\lambda} \\ \varphi_{\nu-1}(\lambda) &= x_0 + s * \ln\left(1 + e^{\varphi_{\nu-2}}\right) \\ \varphi_\nu(\lambda) &= x_0 - s * \ln\left(1 + e^{\varphi_{\nu-2}}\right), \end{aligned} \quad (25)$$

$$F = -T \int_{-\infty}^{+\infty} s\left(\lambda + \frac{1}{\pi} \ln \frac{T}{T_K}\right) \ln\left(1 + e^{\varphi_1(\lambda)}\right) d\lambda, \quad (26)$$

where the Kondo temperature has been introduced as

$$\begin{aligned} T_K &= \omega_c \exp(-\pi f/\mu) \\ &\equiv \Delta_r/\alpha. \end{aligned} \quad (27)$$

For $\mu > \pi/2$ ($\alpha < 1/2$) the seemingly innocent sign change of the driving term alters the structure of the solutions completely. The derivation of the universal equations becomes much more complicated in this case, but is still possible¹³. These were not used in obtaining the numerical results described below, but they served as a useful check on the simpler set of equations (19). We reproduce them, correcting some minor typos in¹³, in Appendix D, together with a comparison of numerical results obtained from them and the simpler set of equations (19). The equations above clearly show that the thermodynamic quantities depend only on the ratios ε/T and $T/T_K \sim T/\Delta_r$. Note, however, that while the parameter f only influences T_K , for each μ (α) one obtains a different set of equations and therefore different

thermodynamic behaviour. Thus two models have essentially the same universal behaviour if and only if their parameter μ (α) is the same. From these considerations immediately follows that the usual RG scaling trajectories correspond to the lines $T_K = \text{const}$ and $\mu = \text{const}$. (The latter requirement also follows from the fact that 2μ turns out to be the anomalous dimension characterizing the high temperature behaviour, which should be scale invariant.) In the small coupling limit one immediately obtains the usual leading logarithmic scaling equations by expanding f and μ in $\rho J_\perp \approx I_\perp$ and $\rho J_z \approx I_z$:

$$\frac{d\rho J_z}{d\ln\omega_c} = -(\rho J_\perp)^2, \quad (28)$$

$$\frac{d\rho J_\perp}{d\ln\omega_c} = -\rho J_\perp \rho J_z, \quad (29)$$

in agreement with Eq. (7).

2. Asymptotic properties

The asymptotic behaviour of various physical quantities can be determined by analyzing Eq. (19). Rewriting Eq. (19) in terms of the quantities ξ_j , $j = 1, \dots, \nu$ defined by

$$\begin{aligned} \xi_j &= \ln[1 + \exp(\frac{\epsilon_j}{T})] \quad (j = 1, \dots, \nu - 1), \\ \xi_\nu &= \ln[1 + \exp(-\frac{\epsilon_\nu}{T})], \end{aligned} \quad (30)$$

one can easily show that in the $\lambda \rightarrow -\infty$ limit the asymptotic solution of the BA equations behaves as

$$\xi_j(\lambda \rightarrow -\infty) = \xi_j^-(x_0) + b_j^-(x_0)e^{\tau\lambda}. \quad (31)$$

with $\tau = 2\mu$. On the other hand, for $\lambda \gg \ln(T/\omega_c)$ ξ_1 vanishes extremely fast and can be approximated by 0. Substituting these into Eq. (26) and using $\mu/\pi = 1 - \alpha$ and $\Delta_r \sim T_K$ one can immediately extract the leading behaviour of the impurity free energy. In the high temperature limit one obtains:

$$\begin{aligned} F(T \gg \Delta_r, \epsilon) &\approx -T \left\{ \ln \frac{\sinh(\epsilon g/T)}{\sinh(\epsilon g/2T)} + \right. \\ &\quad \left. - \left(\frac{\Delta_r}{T}\right)^{2-2\alpha} \left(A + B \left(\frac{\epsilon}{T}\right)^2 \right) \right\}, \end{aligned} \quad (32)$$

$$\begin{aligned} \chi_{sb}(T \gg \Delta_r; \epsilon = 0) &= -\frac{\partial^2 F}{\partial \epsilon^2} \approx \\ &\approx \frac{1}{T} \left(\frac{g^2}{4} - 2B \left(\frac{\Delta_r}{T}\right)^{2-2\alpha} \right), \end{aligned} \quad (33)$$

$$C(T \gg \Delta_r; \epsilon = 0) \sim \left(\frac{\Delta_r}{T}\right)^{2-2\alpha}, \quad (34)$$

where the constants A and B depend only on μ . From these equations it is clear that in order to recover the free impurity spin at high temperatures — unlike the choice $g = (\nu - 1)/\nu$ of Ref. 13 — we have to take the bare value

$g = 1$ for the electronic g -factor. This special choice will influence the Wilson ratio discussed below.

Similarly, for the low temperature regime we obtain:

$$F(\epsilon \ll T \ll \Delta_r) \approx \frac{T^2}{\Delta_r} \left(\frac{\alpha\pi}{6} + \frac{g^2 \epsilon^2}{4\pi T^2} \right), \quad (35)$$

$$\chi_{sb}(T \ll \Delta_r; \epsilon = 0) \approx \frac{1}{\Delta_r} \frac{g^2}{2\pi}, \quad (36)$$

$$C(T \ll \Delta_r; \epsilon = 0) \approx \frac{\pi T \alpha}{3 \Delta_r}, \quad (37)$$

where the numerical constants have been calculated following the same lines as in Ref. 13. Thus at low temperatures the well-known Fermi liquid behaviour is recovered^{33,34}.

3. Susceptibility and Wilson ratio for the Ohmic two-state system

As discussed by Wiegmann and Tsvetlik,¹³ to ensure integrability, an artificial electron-electron interaction has to be introduced. While this interaction has no effect in the course of the solution of the isotropic model, in the anisotropic model it renormalizes the electronic and impurity g -factors:

$$g = 1 \rightarrow \tilde{g} = \frac{1}{\sqrt{\alpha}} = \frac{1}{\sqrt{1 - \mu/\pi}}. \quad (38)$$

This can be most easily checked by calculating the host susceptibility of the AKM, $\chi_{host} = -\partial^2 F_{host}/\partial h^2$, following the lines of Ref. 13. (Here F_{host} is the free energy of the electrons, and is given by an expression similar to Eq. (22) with $f = 0$.) After a tedious calculation one obtains the result that:

$$\chi_{host} = \frac{\chi_{free}}{1 - \mu/\pi} = \frac{\chi_{free}}{\alpha}, \quad (39)$$

where $\chi_{free} = L/(4\pi N)$ denotes the free electron susceptibility (L is the length of the system, N the number of electrons, and $v_F = k_B = 2\mu_B = 1$). Note that the specific heat, $C_{host} = C_{free} = TL\pi/N3$, is completely unaffected by the electron-electron interaction.

We now prove the statement made in Sec. III A, that the impurity contribution to the global susceptibility of the AKM, *obtained from the Bethe Ansatz calculations*, is identical to the susceptibility of the Ohmic two-state system. We denote the bare g -factors of the impurity and conduction electrons in the AKM by g_i and g_e and the corresponding susceptibility of the AKM by $\chi(g_i, g_e)$ ³⁵. Now in the Bethe Ansatz solution, starting with bare values $g_i = g_e = 1$, the renormalizations discussed above imply that the BA susceptibility, $\chi_{BA} \equiv -\partial^2 F/\partial \epsilon^2$, is given by

$$\chi_{BA} = \chi(\tilde{g}_i = \tilde{g}_e = 1/\sqrt{\alpha}) \equiv \chi(g_i = g_e = 1)/\alpha. \quad (40)$$

The dielectric susceptibility of the Ohmic two-state system, χ_{sb} , measures the response to a local electric field and is equal to the impurity susceptibility of the AKM, $\chi(g_i = 1, g_e = 0)$, with the magnetic field coupling only to the impurity spin:

$$\chi_{sb} = \chi(g_i = 1, g_e = 0). \quad (41)$$

This follows from the equivalence of the two models discussed in Appendix A. We now make use of Eq.21 of Ref. 36 (valid for arbitrary T), connecting the impurity susceptibilities of the AKM with arbitrary g -factors. This states that

$$\chi(g_i = g_e = 1) = (1 + 2\frac{\delta}{\pi})^2 \chi(g_i = 1; g_e = 0), \quad (42)$$

where the phase shifts have been defined in Appendix A (note the sign change with respect to Ref. 36). Hence, using (40-41) and Eq. (A16) $\alpha = (1 + 2\frac{\delta}{\pi})^2$, we find that the BA susceptibility is just the susceptibility of the Ohmic two-state system,

$$\chi_{BA}(T, \varepsilon) \equiv -\partial^2 F / \partial \varepsilon^2 = \chi(\tilde{g}_i = \tilde{g}_e = 1/\sqrt{\alpha}) = \chi_{sb}, \quad (43)$$

as stated earlier. This can be further checked by calculating the high temperature Curie susceptibility and the Wilson ratio (from Eqs. (36) and (37)) for which we find

$$\chi_{sb} = \chi_{BA}(T \gg T_K \sim \Delta_r) \approx \frac{1}{4T}, \quad (44)$$

$$R_{sb} = R_{BA} \equiv \lim_{T \rightarrow 0} \frac{C_{free}(T)}{\chi_{free}} \frac{\chi_{BA}}{C(T)} = 2/\alpha, \quad (45)$$

in agreement with exact results obtained for the spin-boson model.³⁷ Furthermore, one can easily check by a bosonization procedure along the Toulouse line⁵⁶ that Eq. (48) is identical with the impurity contribution to the free energy in the presence of a *local* magnetic field applied at the impurity. We note that the above result for the Wilson ratio of the Ohmic two-state system holds for all level asymmetries (local magnetic field in the AKM). Finally, in order to prevent confusion, we state the connection of the above Wilson ratio for the Ohmic two-state system to that usually encountered in the Kondo model. The former is defined using the susceptibility of the Ohmic two-state system χ_{sb} which we showed was equal to the susceptibility χ_{BA} resulting from the BA calculation on the AKM (with an electron-electron interaction to ensure integrability). The susceptibility used in defining the Wilson ratio for magnetic impurities is, however, not $\chi_{BA} = \chi_{sb} = \chi(g_i = 1, g_e = 0)$ but $\chi(g_i = 1, g_e = 1)$. Therefore, in terms of this susceptibility, and using Eq. (42), the corresponding Wilson ratio, R_{akm} , is given by

$$R_{akm} \equiv \lim_{T \rightarrow 0} \frac{C_{free}(T)}{\chi_{free}} \frac{\chi(g_i = g_e = 1)}{C(T)} = 2. \quad (46)$$

The enhancement over the non-interacting value $R = 1$, indicates that the quasiparticles are strongly interacting at low temperatures¹⁴.

4. The Toulouse point: $\alpha = 1/2$

The AKM possesses a so-called Toulouse line^{16,36,56}. Along this line the model can be mapped by a simple unitary transformation to a resonant level model without interaction and can be solved by refermionization. For a dissipative two-state system this line has been shown to correspond to the special value $\alpha = 1/2$ ($\mu = \pi/2$, $\nu = 2$ in the BA solution) separating the coherent and incoherent tunneling regimes.

Along this line the BA solution simplifies enormously too: For $\nu = 2$ only 'one-strings' with parity $v = \pm$ are allowed, and as one can immediately check by using Eq. (B7), the rapidities of the spin-excitations are completely decoupled. Therefore, in the first of Eqs. (19) only the driving term remains and one obtains in the scaling limit:

$$\begin{aligned} \frac{1}{T} \epsilon_1(\lambda) &= -\frac{\omega_c}{T} e^{\pi\lambda} + \frac{g\varepsilon}{T}, \\ \frac{1}{T} \epsilon_2(\lambda) &= \frac{\omega_c}{T} e^{\pi\lambda} + \frac{g\varepsilon}{T}. \end{aligned} \quad (47)$$

Substituting these expressions into Eq. (22) one immediately arrives at

$$\begin{aligned} F &= -\frac{T}{\pi} \int_0^\infty dk \frac{T_K}{k^2 + T_K^2} \ln \{ 1 + 2 \cosh(g\varepsilon/T) e^{-k/T} \\ &\quad + e^{-2k/T} \}, \end{aligned} \quad (48)$$

which coincides with the resonant level result (note the slight difference with respect to the formula 6.2.15 of Ref.¹³). It is straightforward to verify that in the limit $T \rightarrow 0$

$$\chi_{sb} = g^2 / (\pi T_K) \equiv g^2 / 2\pi \Delta_r, \quad \alpha = 1/2$$

and

$$C = \pi T / (3T_K) \equiv \pi T / 6\Delta_r, \quad \alpha = 1/2$$

giving the expected Wilson ratio, $R_{sb} = 2/\alpha = 4$, for the Ohmic two-state system at $\alpha = 1/2$, with R_{sb} as defined above. The high temperature limits $S = \ln 2$ and $\chi_{BA}(T \gg T_K \sim \Delta_r) = g^2 / 4T$ are also easily verified.

IV. NUMERICAL RESULTS AT ALL TEMPERATURES

A. Numerical procedure

The closure of the infinite set of thermodynamic Bethe Ansatz equations to a finite set at rational values of the dissipation strength α can be used to obtain highly accurate results for the thermodynamics. This avoids the truncation errors associated with solving these equations at other values of α . In particular at $\alpha = 1/\nu$ and

$\alpha = 1 - 1/\nu$ we have ν equations. In the numerical procedure we found it more convenient to set up integral equations for new quantities $\xi_j, j = 1, \dots, \nu$ defined by eq. (30)

$$\begin{aligned}\xi_j &= \ln[1 + \exp(\frac{\epsilon_j}{T})] = \ln[1 + \kappa_j], \quad j = 1, \dots, \nu - 1 \\ \xi_\nu &= \ln[1 + \exp(-\frac{\epsilon_\nu}{T})] = \ln[1 + \kappa_\nu],\end{aligned}\quad (49)$$

where the functions $\kappa_j, j = 1, \dots, \nu$ are introduced for later convenience.

The TBA equations then take the form,

$$\begin{aligned}\xi_j(\lambda) &= \ln[1 + \exp(\delta_{j,1}D(\lambda) \\ &\quad + s * (\xi_{j-1} + \xi_{j+1} + \delta_{j,\nu-2}\xi_\nu))], \\ \xi_{\nu-1}(\lambda) &= \ln[1 + \exp(x_0 + s * \xi_{\nu-2})], \\ \xi_\nu(\lambda) &= \ln[1 + \exp(-x_0 + s * \xi_{\nu-2})].\end{aligned}\quad (50)$$

The impurity free energy is given by

$$F(T, \epsilon) = -k_B T \int_{-\infty}^{+\infty} s(\lambda + f/\mu) \xi_1(\lambda, T, \epsilon) d\lambda \quad (51)$$

where $s(\lambda) = (2 \cosh(\pi\lambda))^{-1}$ and f/μ is related to the low energy scale, T_K , of the AKM by Eq. (27)

The Kondo temperature, T_K , is related to the renormalized tunneling amplitude, Δ_r , by $\Delta_r = \alpha T_K$ as discussed in Sec.IIc. The entropy, specific heat and dielectric susceptibility can be obtained by numerically differentiating the Free energy:

$$\begin{aligned}S(T, \epsilon) &= -\frac{\partial F}{\partial T} = \int s(\lambda + f/\mu) \frac{\partial T \xi_1(\lambda, T, \epsilon)}{\partial T} d\lambda \\ C(T, \epsilon) &= -T \frac{\partial^2 F}{\partial T^2} = \int s(\lambda + f/\mu) \frac{\partial^2 T \xi_1(\lambda, T, \epsilon)}{\partial T^2} d\lambda \\ \chi(T, \epsilon) &= -\frac{\partial^2 F}{\partial \epsilon^2} = \frac{g^2}{4T} \int s(\lambda + f/\mu) \frac{\partial^2 \xi_1(\lambda, T, \epsilon)}{\partial x_0^2} d\lambda\end{aligned}$$

A more accurate procedure is to set up integral equations for the derivatives $\partial(T\xi_j)/\partial T$, $\partial\xi_j/\partial x_0$ and $\partial^2\xi_j/\partial x_0^2$. More precisely, we set up integral equations for a new set of functions, E_j, F_j and $G_j = \partial(T\xi_j)/\partial T = \xi_j + T\partial\xi_j/\partial T$ where E_j and F_j are the first and second field derivatives of ξ_j ,

$$E_j \equiv \frac{\partial \xi_j}{\partial x_0} = \frac{\partial \kappa_j / \partial x_0}{1 + \kappa_j}, \quad (52)$$

$$F_j \equiv \frac{\partial^2 \xi_j}{\partial x_0^2} = \frac{\partial^2 \kappa_j / \partial x_0^2}{1 + \kappa_j} - \left[\frac{\partial \kappa_j / \partial x_0}{1 + \kappa_j} \right]^2, \quad (53)$$

and the functions κ_j where defined in (49). Each set of functions $E_j, F_j, G_j, j = 1, \dots, \nu$ then obey coupled linear inhomogeneous integral equations. The equations are,

$$\begin{aligned}E_j &= (1 - e^{-\xi_j}) s * (E_{j-1} + E_{j+1} + \delta_{j,\nu-2}E_\nu) \\ E_{\nu-1} &= (1 - e^{-\xi_{\nu-1}}) (s * E_{\nu-2} + 1), \\ E_\nu &= (1 - e^{-\xi_\nu}) (s * E_{\nu-2} - 1)\end{aligned}\quad (54)$$

for the E_j , with the inhomogeneity appearing in the last two equations. For the F_j we have

$$\begin{aligned}F_j &= Q_j + (1 - e^{-\xi_j}) s * (F_{j-1} + F_{j+1} + \delta_{j,\nu-2}F_\nu) \\ F_{\nu-1} &= Q_{\nu-1} + (1 - e^{-\xi_{\nu-1}}) s * F_{\nu-2}, \\ F_\nu &= Q_\nu + (1 - e^{-\xi_\nu}) s * F_{\nu-2},\end{aligned}\quad (55)$$

with an inhomogeneous term,

$$Q_j = E_j^2 e^{-\xi_j} (1 - e^{-\xi_j})^{-1}.$$

and for the G_j we find

$$\begin{aligned}G_j &= S_j + (1 - e^{-\xi_j}) s * (G_{j-1} + G_{j+1} + \delta_{j,\nu-2}G_\nu) \\ G_{\nu-1} &= S_{\nu-1} + (1 - e^{-\xi_{\nu-1}}) s * G_{\nu-2}, \\ G_\nu &= S_\nu + (1 - e^{-\xi_\nu}) s * G_{\nu-2}\end{aligned}\quad (56)$$

with an inhomogeneous term,

$$S_j = -e^{-\xi_j} \ln e^{-\xi_j} - (1 - e^{-\xi_j}) \ln(1 - e^{-\xi_j}).$$

The numerical procedure is to first solve iteratively for the $\xi_j, j = 1, \dots, \nu$. Using this solution one then iteratively solves for the functions $E_j, F_j, G_j, j = 1, \dots, \nu$ in turn. Fig. 6 shows a graphical representation of these integral equations.

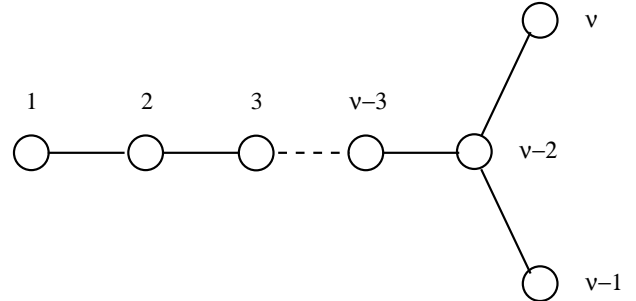


FIG. 6. Graphical representation of the integral equations for the $\xi_j, E_j, F_j, G_j, j = 1, \dots, \nu$.

The entropy and susceptibility are thereby obtained without the need to take any numerical derivatives. Only one derivative is required to obtain the specific heat from the entropy, so we did not set up separate integral equations for the second temperature derivative of $T\xi_1$. Such a procedure has been used for zero field static susceptibilities in³⁸. This approach also overcomes difficulties at large fields (level asymmetries) and low temperatures found in early treatments of similar TBA equations for Kondo systems³⁹ provided one deals with the exponential decrease in the $j = 1$ ($j = \nu$) functions for strong (weak) dissipation respectively. This and further details of the numerical procedure and its accuracy are given in Appendix C.

1. Choice of parameters

The TBA equations were solved for weak dissipation at $\alpha = 1/6, 1/5, 1/4, 1/3$, and for strong dissipation at $\alpha = 2/3, 3/4, 4/5$. The exact closed solution was used to obtain results at the Toulouse point $\alpha = 1/2$. The thermodynamics was calculated at temperatures $t_m = \alpha k_B T_m / \Delta_r = 2^{m/2}$ with $m = -20, -19, \dots, +19, +20$, and for level asymmetries $\tilde{\varepsilon}_n = \alpha \varepsilon_n / \Delta_r = 2^n$ with $n = -4, -3, \dots, +3, +4$ and for the symmetric case $\varepsilon = 0$.

B. Entropy and Specific heat

1. Symmetric case: $\varepsilon = 0$

The entropy of the symmetric two-state system is shown in Fig. 7a as a function of temperature for several values of the dimensionless dissipation strength, α , ranging from weak to strong dissipation. The correct value of the entropy, $S = \ln 2$, is recovered at high temperature for all α . Fig. 7b shows the universal specific heat curves for the dissipative two-state system. As in other strongly correlated systems⁴⁶ we observe a characteristic crossing point for the specific heat curves at a temperature $k_B T^+ / \Delta_r = 0.66 \pm 0.02$. At low temperature the specific heat is given by $C(T) = \alpha \tilde{\gamma}(T/\Delta_r) + b(\alpha)(T/\Delta_r)^3 + \dots$ with a linear coefficient of specific heat $\gamma = \alpha \tilde{\gamma} / \Delta_r$ which vanishes as $\alpha \rightarrow 0$. From the definition of the low energy scale Δ_r in terms of the zero temperature susceptibility and the Wilson ratio (to be discussed below) it follows that $\tilde{\gamma} = \pi/3$ for all α , a useful check on the numerical results. The coefficient $b(\alpha)$ of the T^3 term is negative for $\alpha \geq 1/3$, a special point in the parameter space of the dissipative two-state system.

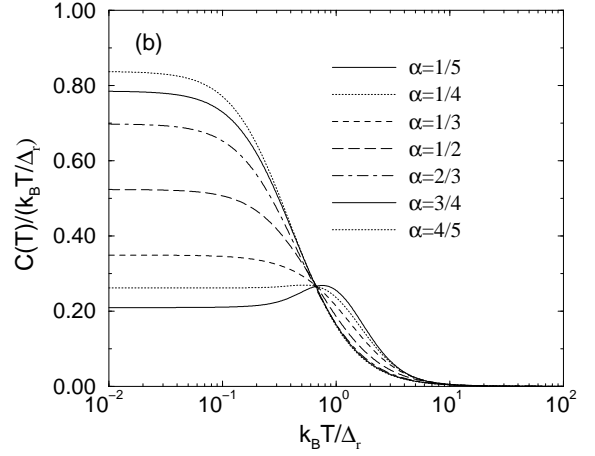
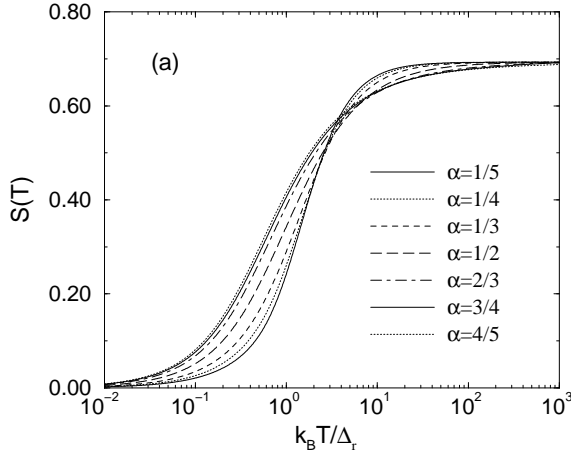
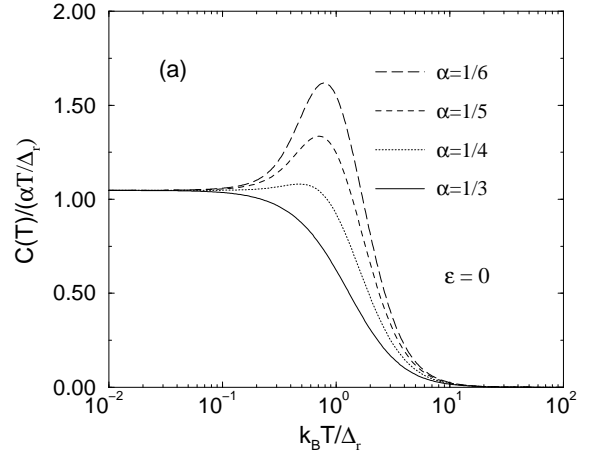


FIG. 7. (a) Entropy, $S(T)$, and (b) specific heats, $C(T)/T$, for the symmetric two-state system ($\varepsilon = 0$) for weak ($\alpha < 1/2$) and strong ($\alpha > 1/2$) dissipation cases. The T^3 coefficient in $C(T)/T$ is negative for $\alpha > 1/3$ and positive for $\alpha < 1/3$.

The significance of $\alpha = 1/3$ is best seen in the context of the dynamics of the two-state system, where it corresponds to the value of the dissipation strength at which the frequency, $\Omega(\alpha)$, of tunneling oscillations (manifested in real time correlation functions) becomes equal to the decay rate, $\Gamma(\alpha)$, of these oscillations, i.e. $\Omega(\alpha = 1/3) = \Gamma(\alpha = 1/3)$ (or the quality factor $Q(\alpha) = \Omega(\alpha)/\Gamma(\alpha)$ becomes unity)^{4,25}. For dissipation $\alpha < 1/3$ we have $\Omega(\alpha) > \Gamma(\alpha)$ and the well defined oscillatory mode appears to be reflected in the characteristic peak in the specific heat $C(T)/T$ ⁴⁷.



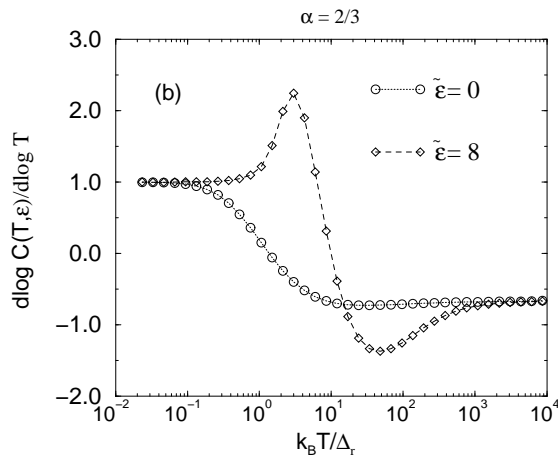


FIG. 8. (a) Specific heat, $C(T)/(\alpha T/\Delta_r)$, showing the development of the peak at $k_B T \approx \Delta_r$ for $\alpha < 1/3$ and $\epsilon = 0$. $\lim_{T \rightarrow 0} C(T)/(\alpha T/\Delta_r) = \tilde{\gamma} = \pi/3 = 1.04719755$ is recovered to 5 decimal places. (b) the logarithmic derivative, $d \log C(T, \epsilon)/d \log T$, at $\alpha = 2/3$ for the symmetric ($\epsilon = 0$) and asymmetric ($\epsilon/\Delta_r = 8$) cases. The approach to the expected power law $C(T) \sim (\Delta_r/k_B T)^\delta$ with $\delta = 2\alpha - 2 = 2/3$ for $\alpha = 2/3$ is found at high temperatures for both cases. For the asymmetric system the power law arises at higher temperature corresponding to the higher low energy scale behaving as $\sqrt{\epsilon^2 + \Delta_r^2} > \Delta_r$ for $\epsilon \gg \Delta_r$.

The peak in $C(T)/T$ for $\alpha < 1/3$ is shown in more detail in Fig. 8a and is reminiscent of the activated behaviour seen in non-interacting two-level systems. Since the excitation spectrum of the Ohmic two-state system is gapless for all $\alpha > 0$, there is no exponential suppression of $C(T)/T$ at low $k_B T < \Delta_r$ as with non-interacting two-level systems. The linear specific heat persists at low temperature and the system remains strongly interacting down to $T = 0$ as is also clear from the value of the Wilson ratio (see later). At high temperatures $k_B T \gg \Delta_r$ the specific heat vanishes according to a power law, $C(T) \sim (\Delta_r/k_B T)^{2-2\alpha}$ with an α dependent power in accordance with the asymptotic result given by Eq.(34) and in¹⁸. This is shown in Fig. 8b and we see that, as for low temperatures, the behaviour at high temperatures is again drastically different to the behaviour of a non-interacting two-level system which shows $C(T) \sim (\Delta_0/k_B T)^2$ for $k_B T \gg \Delta_0$ with Δ_0 the bare tunneling matrix element. The limit $\alpha \rightarrow 1^-$ corresponds to the weak coupling Kondo model. For weak coupling, $\rho J_\perp, \rho J_\parallel \ll 1$, the exchange operators in the AKM become marginal (see above discussion of the Anderson-Yuval scaling equations) and consequently the high temperature properties acquire logarithmic corrections leading to a slow approach of the thermodynamic quantities to their high temperature limits¹⁷ (this can be seen in the entropy in Fig. 7a and more clearly in the results for the susceptibility to be described in the next section).

2. Asymmetric case: $\epsilon > 0$

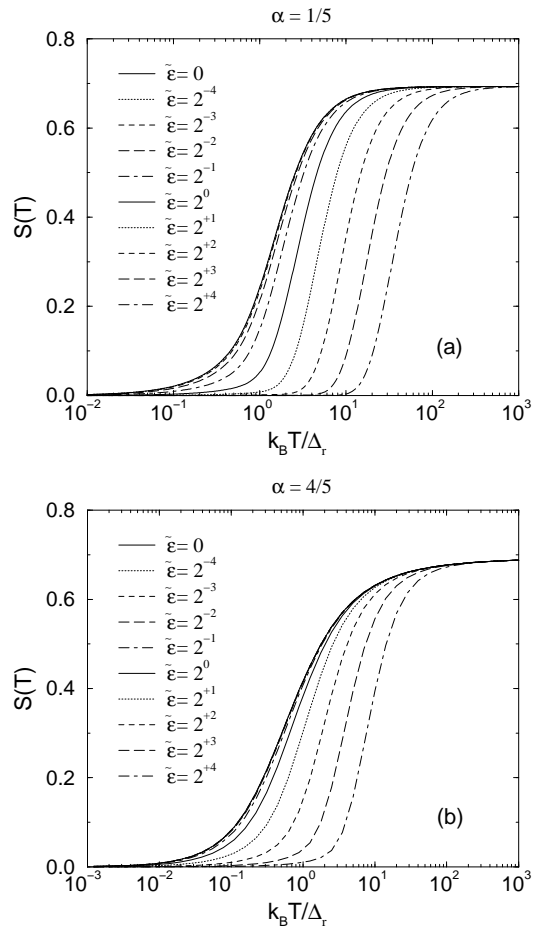


FIG. 9. Entropy, $S(T)$, for the asymmetric two-state system for a range of asymmetries at (a) $\alpha = 1/5$ and (b) $\alpha = 4/5$.

We now turn to the asymmetric two-state system. Fig. 9 shows the temperature dependence of the entropy for different level asymmetries at $\alpha = 1/5$ and $\alpha = 4/5$. The correct high temperature limit $S = \ln 2$ is recovered for all level asymmetries and dissipation strengths. As for the symmetric case, we see again that the entropy approaches its high temperature limit more slowly for strong dissipation than for weak dissipation, again a result of increasing marginality of the interactions with increasing α at the high energy fixed point.

In Fig. 10–11 we show the specific heats for different level asymmetries and dissipation strengths. The specific heat remains linear at low temperature, $C(T, \epsilon) \sim \gamma T$, for all level asymmetries. The linear coefficient $\gamma \sim 1/\Delta_r$ is reduced with increasing asymmetry ϵ , a consequence of the increasing low energy scale with increasing ϵ , $\Delta_r \rightarrow \sqrt{\Delta_r^2 + \epsilon^2}$. We see that a sufficiently large asymmetry eventually leads to a peak in $C(T)/T$ for all dissipation strengths, but that for such a peak to form requires a sizeable asymmetry for $\alpha > 1/3$.

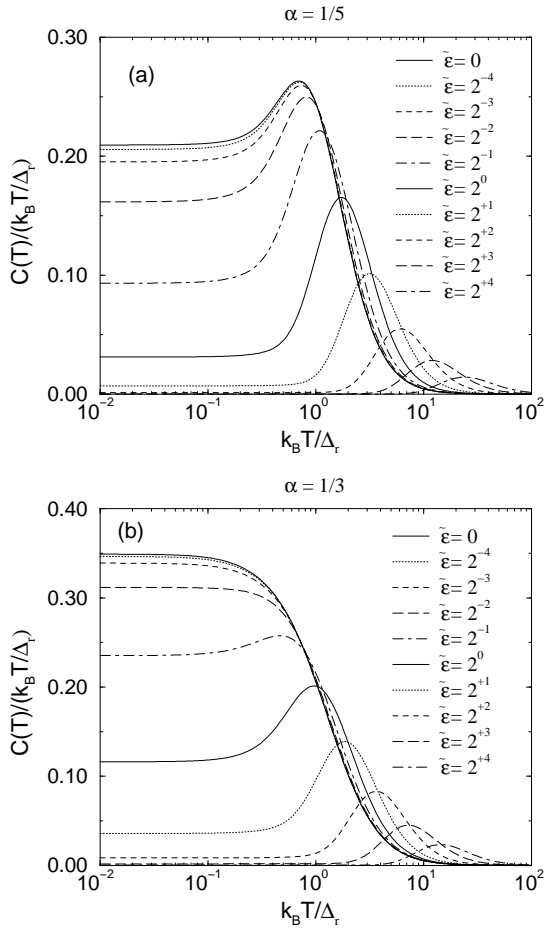


FIG. 10. Specific heats, $C(T)/T$, for the asymmetric two-state system for a range of asymmetries, and some typical cases for weak dissipation, (a) $\alpha = 1/5$, (b) $\alpha = 1/3$.

It is important to note that even for large asymmetries, the shape of the specific heat curves is still different to those of a non-interacting two-level system: at low temperature the specific heat remains linear rather than exponential and at high temperature the asymptotic behaviour of $C(T)$ is not the non-interacting $1/T^2$ but instead behaves as $1/T^{2-2\alpha}$ as shown analytically for $\varepsilon = 0$ and numerically for $\varepsilon > 0$ in Fig. 8. Only for $\alpha \ll 1$ do we expect the specific heat to be reasonably described by the non-interacting result, and then only outside the Fermi liquid regime $k_B T > \Delta_r$.

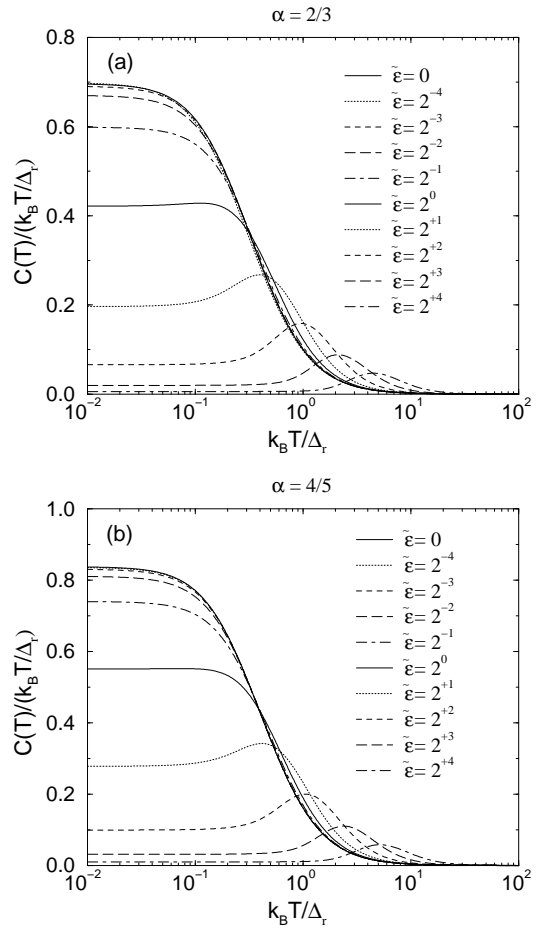


FIG. 11. Specific heats, $C(T)/T$, for the asymmetric two-state system for a range of asymmetries, and some typical cases for strong dissipation, (a) $\alpha = 2/3$, (b) $\alpha = 4/5$.

C. Dielectric Susceptibility

1. Symmetric case: $\varepsilon = 0$

Fig. 12 shows that the dielectric susceptibility of the dissipative two-state system remains finite down to $T = 0$ for all dissipation strengths $\alpha < 1$. This is also shown in Fig. 13 together with the Fermi liquid T^2 corrections at $k_B T \ll \Delta_r$ given by Eq.(36), $\chi_{sb}(T) = \chi_{sb}(0)(1 - c(\alpha)(k_B T / \Delta_r)^2)$. By our definition $\chi_{sb}(T = 0) = 1/2\pi\Delta_r$, we have that $\Delta_r \chi_{sb}(T = 0) = 1/2\pi = 0.1591549$ which is reproduced by our numerical solution to 5 decimal places in all cases (Fig. 13). In contrast to the specific heat, $C(T)/T$, the susceptibility is a monotonically decreasing function of temperature for all dissipation strengths. There is no signature of the onset of activated behaviour in the susceptibility as there was for $\alpha < 1/3$ in $C(T)/T$. As we shall see below, a finite temperature peak in χ_{sb} only arises when there is a finite level asymmetry. The dielectric susceptibility looks, superficially, like that for a non-interacting system, however the universal scaling curves depend sensitively on α ,

as can be seen in Fig. 12, so that this resemblance is misleading.

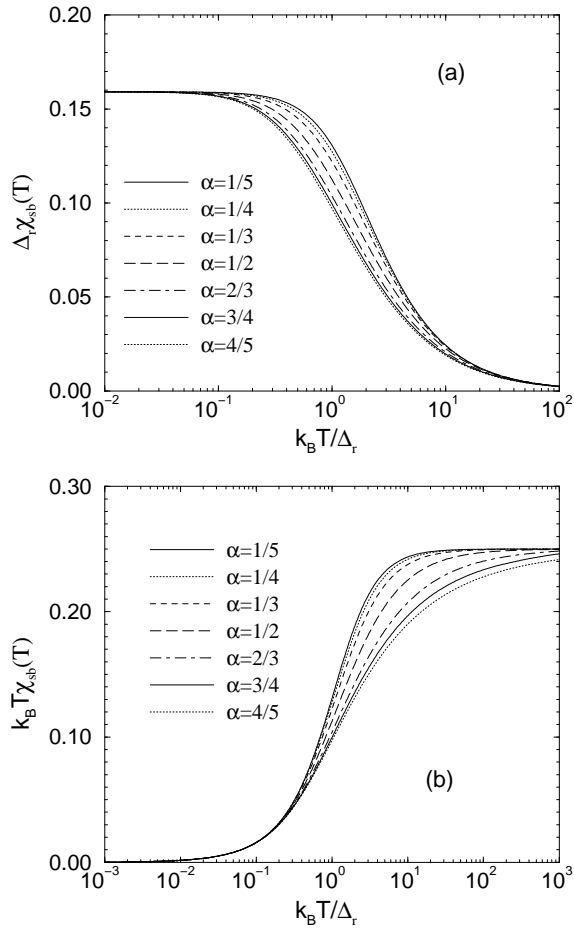


FIG. 12. Dielectric susceptibility, $\chi_{sb}(T)$, for the symmetric two-state system ($\varepsilon = 0$) for weak ($\alpha < 1/2$) and strong ($\alpha > 1/2$) dissipation cases. The susceptibility is finite at $T = 0$ with $\Delta_r(\alpha)\chi(T=0) = 1/2\pi$ in all cases as seen in (a) and attains its free-spin value of $1/4T$ at high temperatures $k_B T \gg \Delta_r$, as seen in (b).

The strong renormalization of the tunneling amplitude $\Delta_r/\omega_c \sim (\Delta_0/\omega_c)^{1/(1-\alpha)}$ as $\alpha \rightarrow 1^-$ gives rise to strongly renormalized dielectric susceptibilities at low temperatures and strong dissipation ($\chi_{sb}(T=0) = 1/2\pi\Delta_r$). The approach of the susceptibility to its free spin value of $1/4$ at $k_B T \gg \Delta_r$ at high temperatures (Fig. 12b) is governed by power laws with exponents which are functions of the dissipation strength as given by Eq.(33), $k_B T\chi_{sb}(T) \approx 1/4 - 2B(\Delta_r/k_B T)^{2-2\alpha}$, and verified in Fig. 14. The approach to the free spin value becomes slower as $\alpha \rightarrow 1^-$ and eventually logarithmic corrections to the susceptibility set in (see Fig. 12b).

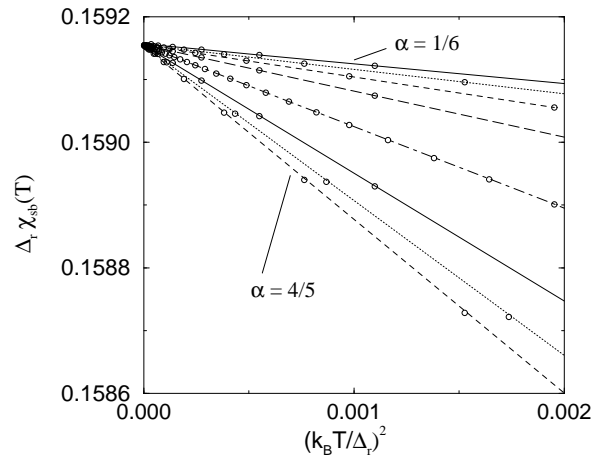


FIG. 13. The T^2 Fermi liquid corrections to the dielectric susceptibility at low temperatures for the symmetric case and $\alpha = 1/6, 1/5, \dots, 3/4, 4/5$.

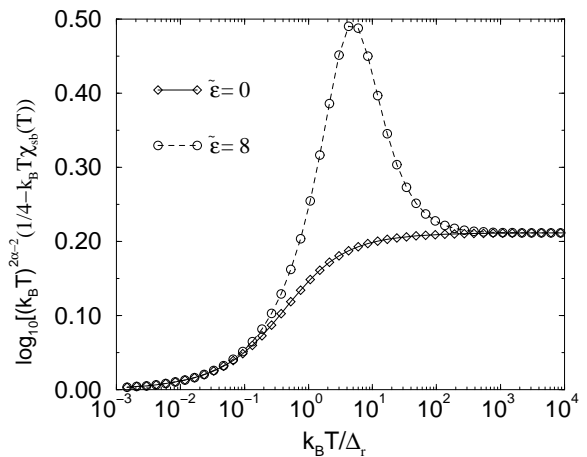


FIG. 14. High temperature corrections to the dielectric susceptibility for $\alpha = 2/3$ for $\tilde{\varepsilon} = 0$ and $\tilde{\varepsilon} = 8$. $\lim_{T \rightarrow \infty} \log_{10}[(k_B T)^{2\alpha-2}(1/4 - k_B T\chi_{sb}(T))] = \log_{10}(2B)$

2. Asymmetric case: $\varepsilon > 0$

The dielectric susceptibility in the presence of a level asymmetry is shown in Fig. 15–16. For all dissipation strengths we see that a sizeable asymmetry of the order of Δ_r is required to give a finite temperature peak in χ_{sb} . The approach of the susceptibility to its high temperature limit of $1/4T$ is governed by the same power laws as those found for the symmetric case and verified in Fig. 14.

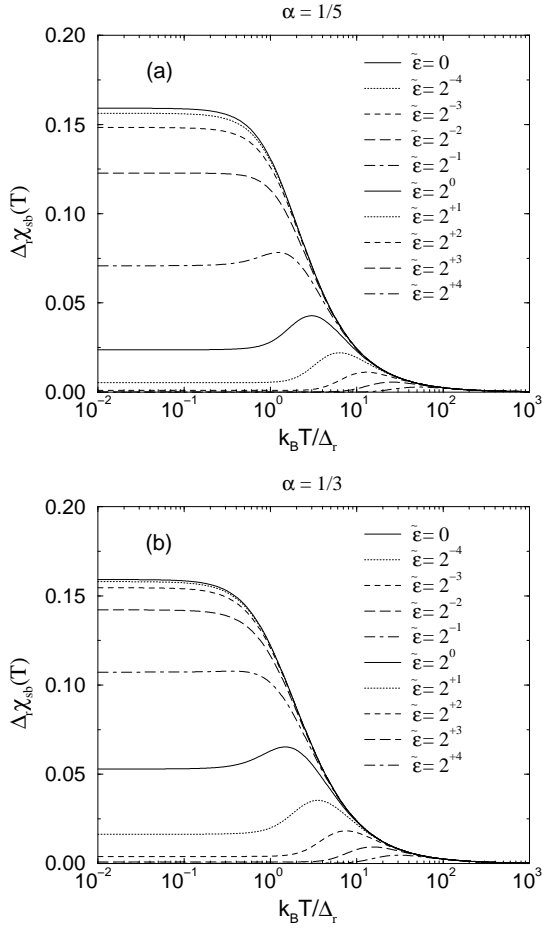


FIG. 15. Dielectric susceptibility, $\chi_{sb}(T)$, for a range of asymmetries and some typical cases of weak dissipation, (a) $\alpha = 1/5$, (b) $\alpha = 1/3$.

3. Wilson ratio

The Wilson ratio for the Ohmic two-state model, R_{sb} , was defined earlier together with the usual Wilson ratio, R_{akm} , for the AKM. These take the values $2/\alpha$ and 2 respectively and are valid for both the symmetric and asymmetric cases (i.e. in both zero and finite fields for the Kondo model). The Wilson ratio served as a useful check on our numerical solution, which recovered it with an accuracy of not less than 4 decimal places for all α and ϵ .

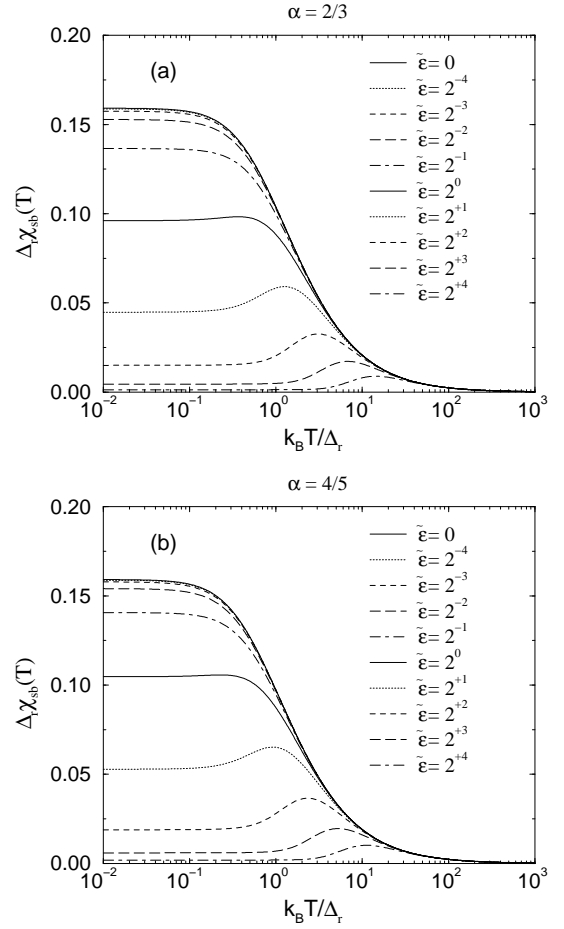


FIG. 16. Dielectric susceptibility, $\chi_{sb}(T)$, for a range of asymmetries and some typical cases of strong dissipation, (a) $\alpha = 2/3$, (b) $\alpha = 4/5$.

V. SUMMARY AND DISCUSSION

In the present paper we studied the thermodynamics of a TSS with Ohmic dissipation by exploiting a mapping between the DTSS and the anisotropic Kondo model, and solving the Bethe Ansatz equations derived by Wiegman and Tsvetlik for the latter. Treating the BA equations in a careful way we were able to calculate essentially exactly the specific heat and the susceptibility of the DTSS for all temperatures and level asymmetries in the delocalized phase of the DTSS, characterized by dissipation strengths $0 < \alpha < 1$. The Bethe Ansatz solution makes the universal properties of the DTSS clear: thermodynamic quantities are universal functions of two variables, $k_B T/\Delta_r$ and $\epsilon/k_B T$ for all $\alpha < 1$. In the limit $\alpha \rightarrow 1^-$ these functions reduce to those of the usual isotropic $S = 1/2$ Kondo model, which is seen as a special point in the parameter space of the DTSS¹⁷. The well known logarithmic corrections to physical quantities for $\alpha \rightarrow 1^-$ at high temperatures $k_B T \gg \Delta_r$ give way to power law corrections away from $\alpha = 1$. We determined these power laws both analytically and numerically for all $\alpha < 1$ at

finite ε . In the context of the RG the change from logarithmic to power law corrections to physical quantities at high temperature indicates that the tunneling term in the Hamiltonian changes from being marginally relevant (about the high energy fixed point) at $\alpha = 1$ to relevant at $\alpha < 1$ as discussed in Sec. II C. At low temperature $k_B T \ll \Delta_r$ the thermodynamics of the DTSS is that of a renormalized local Fermi liquid with an enhanced linear specific heat $C(T) \sim \alpha k_B T / \Delta_r$, and an enhanced, but finite, dielectric susceptibility at $T = 0$, $\chi_{sb}(T = 0) = 1/2\pi\Delta_r$. The renormalizations increase dramatically as $\alpha \rightarrow 1^-$ due to the strong renormalization of the low energy scale $\Delta_r/\omega_c \sim (\Delta/\omega_c)^{1/(1-\alpha)}$.

We have shown that the characteristic thermodynamic properties of the DTSS change smoothly as one increases the dissipation strength from $\alpha \ll 1/2$ to $1 > \alpha > 1/2$, corresponding to weak and strong dissipations, respectively. In the former case, where the DTSS displays coherent oscillations between its two positions⁵, we find the expected tendency towards activated behaviour in the specific heat. A clear signal of this behaviour is the appearance of a peak in $C(T)/T$ at the renormalized tunneling amplitude Δ_r . Such a peak is absent for dissipations $\alpha > 1/3$ in the symmetric case. A finite level asymmetry accentuates the tendency towards activated behaviour and always gives rise to a finite temperature peak in $C(T)/T$ at temperature $k_B T = \tilde{\Delta}_r \sim \sqrt{\Delta_r^2 + \varepsilon^2}$ provided $\varepsilon \geq \Delta_r$. For strong dissipation $\alpha > 1/2$, the specific heat is qualitatively similar to that of isotropic $S = 1/2$ Kondo systems and shows a monotonically decreasing $C(T)/T$ with increasing temperature. The dielectric susceptibility of the DTSS was calculated at all dissipation strengths, level asymmetries and temperatures for the first time. For the symmetric case we found that this quantity decreases monotonically with increasing temperature for all dissipation strengths and develops a finite temperature peak only for sufficiently large level asymmetries (of the order of Δ_r).

The Ohmic two-state system is a generic model capable of describing a large number of different physical systems. Previous theoretical and experimental work on such systems has, however, largely focussed on the dynamic properties. Given the detailed understanding which we now have of the thermodynamics, it may be worthwhile to consider also thermodynamic measurements on Ohmic two-state systems. We therefore briefly mention below some possibilities where our results could be directly tested.

One of the possible physical realizations is provided by two-level systems in metals. Amorphous metals are not the best candidates, however, since in these materials a broad distribution of DTSS's with very different physical parameters occur. Therefore, to calculate their contribution to the thermodynamic properties one should average over them. This averaging is not impossible, but would require solving the BA equations for arbitrary values of α , something which could be implemented by using further results of Ref¹³. In addition one would require the

form of the TSS distribution. Better candidates are H tunneling in Nb⁴⁸ and metallic materials with tunneling centers formed by substitutional impurities, such as $Pb_{1-x}Ge_xTe$ ⁴⁹. Good quality single crystals can be produced from the latter alloy. The Germanium ions form identical eight-state systems, which couple to the conduction electrons. Applying external stress on the sample one can reduce the degeneracy of the lowest lying states to two. Since in this case the DTSS's have approximately identical parameters for weak concentrations their individual thermodynamic properties can be observed by measuring the sample's macroscopic properties.

Another possible candidate for thermodynamic measurements is provided by a SQUID. In this case the energy difference between the two flux states of the SQUID can be easily tuned by an external magnetic field. Measuring the average flux $\langle \Phi \rangle$ as a function of the asymmetry energy one can readily determine the susceptibility $\chi \sim \partial \langle \Phi \rangle / \partial B$ that can directly be compared to our calculations.

Finally, the results we have obtained for the thermodynamics of the anisotropic Kondo model may have some relevance to the problem of an isotropic $S = 1/2$ Kondo impurity in a Luttinger liquid. Schiller and Ingersent⁵² have shown that a $S = 1/2$ Kondo impurity in a modified Luttinger liquid consisting only of left-moving spin-down electrons and right-moving spin-up electrons can be mapped exactly onto the AKM. It is clear that in a more realistic description of the Luttinger liquid that this exact mapping will only be approximate, nevertheless we expect that some of the general trends in the thermodynamic properties of a $S = 1/2$ Kondo impurity in an interacting system should be captured by such a mapping onto the AKM or equivalently onto the Ohmic two-state system. The strength, U , of the Coulomb interaction can then be related⁵² to J_{\parallel} in the AKM and hence to the dissipation strength α in the Ohmic two-state system. The non-interacting system with $U = 0$ corresponds to $\alpha = 1$ and $U \rightarrow \infty$ corresponds to $\alpha = 0$. Within such a picture we therefore expect, from the results of this paper, that the thermodynamic scaling functions of an isotropic $S = 1/2$ Kondo impurity in a Luttinger liquid will change continuously with increasing Coulomb interaction U (or decreasing dissipation strength α). At low temperature the thermodynamics of such systems should be similar to that of a local Fermi liquid, as recently discussed in⁵³. For sufficiently large U (i.e. sufficiently small α), $C(T)/T$ may develop a finite temperature peak at $k_B T \sim \Delta_r \sim T_K$ in analogy to our findings for the Ohmic two-state system. Such a peak could then be taken as a signature of the Kondo effect in a strongly interacting system. The unusual heavy fermion behaviour of $Nd_{2-x}Ce_xCuO_4$, e.g. the non-monotonic behaviour of $C(T)/T$ ⁵⁴, may be consistent with such an interpretation. Strong interactions have also been invoked to explain this behaviour in Ref.⁵⁵. Other, more conventional explanations, such as lattice coherence effects, cannot be ruled out however.

The approach we have developed in this paper can be extended to more complicated models of two-level systems coupled Ohmically to an environment. The effect of indirect or electron-assisted tunneling processes^{11,57} on the thermodynamics of two-level systems in metals will be studied in a future publication.

ACKNOWLEDGMENTS

The authors are grateful to N. Andrei and A.M. Tsvelik for useful discussions. We are grateful also to C. Roth for help with Bosonization in Appendix A. This research has been supported by the Hungarian Grant Nos. OTKA T026327, OTKA F016604, and the U.S-Hungarian Joint Fund No. 587. G. Z. has been supported by the Magyary Zoltán Foundation and grant No. DE-FG03-97ER45640 of the U.S DOE Office of Science, Division of Materials Research. T. A. C. thanks the Deutsche Forschungsgemeinschaft for financial support and the hospitality of the Max Planck Institut für Physik Komplexe Systeme, Dresden and the Centre for Electronic Correlations and Magnetism, University of Augsburg, Germany, where part of this research was carried out.

APPENDIX A: EQUIVALENCE OF THE AKM TO THE OHMIC TWO-STATE SYSTEM

1. Bosonization of free fermions

Consider first the free fermion Hamiltonian,

$$H_0 = \sum_{k\mu} \varepsilon_k c_{k\mu}^\dagger c_{k\mu}. \quad (\text{A1})$$

We take a linear dispersion relation for the conduction electrons, $\varepsilon_k = v_F k$, and measure k relative to the Fermi wavenumber k_F . We introduce fermion fields $\psi_\mu(x)$ via a Fourier series,

$$\psi_\mu(x) = L^{-1/2} \sum_k e^{-ikx} c_{k\mu} \quad (\text{A2})$$

with wavenumbers $k = 2\pi n/L, n = 0, \pm 1, \dots$ for periodic boundary conditions appropriate to a finite system of length L . The density of states per spin direction is given by $\rho = 1/2\pi v_F$. The kinetic energy can then be written as,

$$H_0 = v_F \sum_{k,\mu} k c_{k\mu}^\dagger c_{k\mu} = i v_F \int_{-L/2}^{+L/2} \psi_\mu^\dagger(x) \partial_x \psi_\mu(x) dx \quad (\text{A3})$$

The fields $\psi_\mu(x)$ are expressed in terms of hermitian bosonic fields $\varphi(x)$ in the standard way,

$$\psi_\mu(x) = (2\pi a)^{-1/2} F_\mu e^{-i\varphi_\mu(x)} \quad (\text{A4})$$

where a is a lattice spacing, required for obtaining convergent momentum sums. The F_μ are the Klein factors required to ladder between states with different fermion number, and to ensure the correct anticommutation relations for the fermion fields^{29,50}, and

$$\varphi_\mu(x) = \phi_\mu(x) + \phi_\mu^\dagger(x), \quad (\text{A5})$$

with the bosonic fields ϕ, ϕ^\dagger given by

$$\phi_\mu^\dagger(x) = (\phi_\mu(x))^\dagger \equiv - \sum_{q>0} n_q^{-1/2} e^{iqx} a_{q\mu}^\dagger e^{-aq/2}. \quad (\text{A6})$$

The a_q, a_q^\dagger , defined for $q > 0$, satisfy boson commutation relations with $n_q = (qL/2\pi)^{1/2}$, and are given by,

$$a_{q\mu}^\dagger = (a_{q\mu})^\dagger = i n_q^{-1/2} \sum_k c_{k+q\mu}^\dagger c_{k\mu} \quad (\text{A7})$$

It is convenient to introduce spin and charge density operators in place of $a_{q\uparrow}, a_{q\downarrow}$ as follows:

$$a_{qC} = \frac{1}{\sqrt{2}} (a_{q\uparrow} + a_{q\downarrow})$$

$$a_{qS} = \frac{1}{\sqrt{2}} (a_{q\uparrow} - a_{q\downarrow}).$$

The corresponding hermitian fields are,

$$\varphi_C = \frac{1}{\sqrt{2}} (\varphi_\uparrow + \varphi_\downarrow)$$

$$\varphi_S = \frac{1}{\sqrt{2}} (\varphi_\uparrow - \varphi_\downarrow),$$

with commutation relations,

$$[\varphi_C(x), \varphi_S(x')] = 0, \quad (\text{A8})$$

$$[\varphi_{C,S}(x), \partial_{x'} \varphi_{C,S}(x')] = 2\pi i \delta(x - x') \quad (\text{A9})$$

In terms of these we have for the fields and densities,

$$\psi_{C,S}(x) \equiv \frac{F_{C,S}}{\sqrt{2\pi a}} e^{-i\varphi_{C,S}(x)} \quad (\text{A10})$$

$$\rho_{C,S}(x) \equiv \frac{1}{\sqrt{2}} \psi_{C,S}^\dagger(x) \psi_{C,S}(x) = \frac{1}{2\pi\sqrt{2}} \partial_x \varphi_{C,S}(x) \quad (\text{A11})$$

2. Transformation to the Ohmic spin-boson model

We start with the anisotropic Kondo model

$$H_{AKM} = H_0 + H_\perp + H_\parallel \quad (\text{A12})$$

with H_0 as above and,

$$H_{\perp} = \frac{J_{\perp}}{2} \sum_{k,k'} (c_{k\uparrow}^{\dagger} c_{k'\downarrow} S^{-} + c_{k\downarrow}^{\dagger} c_{k'\uparrow} S^{+})$$

$$H_{\parallel} = \frac{J_{\parallel}}{2} \sum_{k,k'} (c_{k\uparrow}^{\dagger} c_{k'\uparrow} - c_{k\downarrow}^{\dagger} c_{k'\downarrow}) S_z$$

In terms of $\varphi_{C,S}$, we can write,

$$\begin{aligned} H_0 &= v_F \sum_{q>0} q (a_{q\uparrow}^{\dagger} a_{q\uparrow} + a_{q\downarrow}^{\dagger} a_{q\downarrow}) \\ &= \frac{v_F}{2} \int_{-L/2}^{+L/2} \frac{dx}{2\pi} : (\partial_x \varphi_C(x))^2 + (\partial_x \varphi_S(x))^2 : \\ H_{\parallel} &= \frac{J_{\parallel}}{2} S_z (\psi_{\uparrow}^{\dagger}(0) \psi_{\uparrow}(0) - \psi_{\downarrow}^{\dagger}(0) \psi_{\downarrow}(0)) \\ &= \frac{J_{\parallel}}{2} S_z \frac{1}{2\pi} \sqrt{2} \partial_x \varphi_S(0) \\ H_{\perp} &= \frac{J_{\perp}}{2} (\psi_{\uparrow}^{\dagger}(0) \psi_{\downarrow}(0) S^{-} + \psi_{\downarrow}^{\dagger}(0) \psi_{\uparrow}(0) S^{+}) \\ &= \frac{J_{\perp}}{4\pi a} \left(e^{i\sqrt{2}\varphi_S(0)} F_{\uparrow} F_{\downarrow}^{\dagger} S^{-} + e^{-i\sqrt{2}\varphi_S(0)} F_{\downarrow} F_{\uparrow}^{\dagger} S^{+} \right) \end{aligned}$$

We note that φ_C (which commutes with φ_S) does not couple to the impurity and only gives a contribution to the kinetic energy.

a. Canonical transformation on the bosonized Model

We show that the unitary transformation $U = \exp(i\sqrt{2}S_z\varphi_S(0))$ applied to H_{AKM} gives the spin-boson Hamiltonian, H_{SB} , for Ohmic dissipation, i.e. that $UH_{AKM}U^{\dagger} = H_{SB}$. We use the Baker-Hausdorff formula $e^{-B}Ae^B = A + [A, B]$ with $[A, B]$ a c-number and the commutation relations for φ_C, φ_S , to obtain,

$$\begin{aligned} UH_0U^{\dagger} &= H_0 - \sqrt{2}v_F S_z \left. \frac{\partial \varphi_S}{\partial x} \right|_{x=0} \\ &= H_0 - \sqrt{2}v_F S_z \\ &\quad \times \sum_q \sqrt{\frac{2\pi q}{L}} (ia_{qS} + (ia_{qS})^{\dagger}) e^{-aq/2}, \\ UH_{\parallel}U^{\dagger} &= H_{\parallel} + \text{constant}, \\ UH_{\perp}U^{\dagger} &= \frac{J_{\perp}}{4\pi a} (e^{i\sqrt{2}\varphi_S(0)} F_{\uparrow} F_{\downarrow}^{\dagger} U S^{-} U^{\dagger} \\ &\quad + e^{-i\sqrt{2}\varphi_S(0)} F_{\downarrow} F_{\uparrow}^{\dagger} U S^{+} U^{\dagger}). \end{aligned}$$

On using the identities,

$$\begin{aligned} U S^{-} U^{\dagger} &= e^{-i\sqrt{2}\varphi_S(0)} S^{-}, \\ U S^{+} U^{\dagger} &= e^{i\sqrt{2}\varphi_S(0)} S^{+}, \end{aligned}$$

and the representation, $\frac{1}{2}\sigma^{+} = F_{\downarrow} F_{\uparrow}^{\dagger} S^{+}$, $\sigma^{-} = (\sigma^{+})^{\dagger}$ and $\frac{1}{2}\sigma_z = S_z$, of the Pauli spin operators, the term $UH_{\perp}U^{\dagger}$ becomes,

$$UH_{\perp}U^{\dagger} = J_{\perp} \frac{1}{4\pi a} \sigma_x. \quad (\text{A13})$$

b. Identification of the parameters of the Kondo Hamiltonian with those of the Spin-boson Hamiltonian

We notice that a_{qC} does not couple to the impurity so we write $a_q = ia_{qS}$ and omit the charge density operators to obtain the Hamiltonian for the spin density excitations,

$$\begin{aligned} H_{SB} &= \frac{J_{\perp}}{4\pi a} \sigma_x + v_F \sum_q q a_q^{\dagger} a_q \\ &\quad + \left(\frac{J_{\parallel}}{4\pi} - v_F \right) \sqrt{2} \frac{\sigma_z}{2} \sum_{q>0} \sqrt{\frac{2\pi q}{L}} (a_q + a_q^{\dagger}) e^{-aq/2}. \end{aligned}$$

This is precisely the spin-boson model,

$$H_{SB} = \sum_{q>0} \omega_q a_q^{\dagger} a_q - \frac{\Delta}{2} \sigma_x + \frac{q_0}{2} \sigma_z \sum_q \frac{C_q}{\sqrt{2m_q\omega_q}} (a_q + a_q^{\dagger})$$

with $\omega_q = v_F q$ and a spectral function for the harmonic oscillators,

$$J(\omega) = \frac{\pi}{2} \sum_q \frac{C_q^2}{m_q \omega_q} \delta(\omega - \omega_q) = \frac{2\pi\alpha}{q_0^2} \omega e^{-\frac{\omega}{\omega_c}},$$

provided one chooses,

$$\frac{C_q}{\sqrt{m_q}} = -\sqrt{\alpha} \frac{2}{q_0} \left(\frac{2\pi v_F}{L} \right)^{1/2} \omega_q e^{-\frac{\omega_q}{2\omega_c}},$$

with a cutoff,

$$\omega_c = \frac{v_F}{a}.$$

One can identify the parameters,

$$-\frac{\Delta}{2} = \frac{J_{\perp}}{4\pi a}$$

and

$$-\sqrt{\alpha} = \frac{J_{\parallel}}{4\pi v_F} - 1,$$

which, together with the density of states (per spin) of the conduction electrons, $\rho = 1/2\pi v_F$, and the above definition of ω_c , result in the following identification of the dimensionless couplings of the two models,

$$\frac{\Delta}{\omega_c} = -\rho J_{\perp} \quad (\text{A14})$$

$$\alpha = \left(1 - \frac{1}{2}\rho J_{\parallel} \right)^2 \quad (\text{A15})$$

The sign of J_{\perp} (or Δ) plays no role and we may choose $\Delta/\omega_c = +\rho J_{\perp} > 0$.

We remark here that the precise form of Eq. (A15) depends on the specific regularization scheme used. Within the framework of Abelian bosonization the coupling J_{\parallel} is

directly proportional to the phase shifts, $\rho J_{\parallel} = 4\pi/\delta$.⁵¹ For a finite-band model with cut-off ω_c , the expression for α in terms of ρJ_{\parallel} the phase shift is given by $\delta = -\arctan(\pi\rho J_{\parallel}/4)$, and Eq. (A15) takes the more general form:

$$\alpha = \left(1 + \frac{2}{\pi}\delta\right)^2. \quad (\text{A16})$$

APPENDIX B: DERIVATION OF THE THERMODYNAMICAL BETHE ANSATZ EQUATIONS

1. Bethe Ansatz equations for finite system sizes

To construct the Bethe Ansatz (BA) solution of the model one first rewrites the AKM Hamiltonian Eq. (2) in coordinate space as:

$$H = \sum_{j=1}^{N_e} \left\{ -i\partial_j + \frac{1}{2}\delta(x_j) [I_z \sigma_j^z S^z + I_{\perp} (\sigma_j^+ S^- + \text{h.c.})] \right\}, \quad (\text{B1})$$

where x_j and $\vec{\sigma}_j$ denote the coordinate and spin of conduction electron j , ($j = 1, \dots, N_e$), and $\vec{S} = \vec{\sigma}_0/2$ is the impurity spin. The explicit relationship between the dimensionless couplings $I_{z,\perp}$ and the J 's in Eq. (2) is not straightforward and depends on the specific regularization and cutoff scheme used in the original model and the BA approach. For small couplings $I_z \approx J_z$ and $I_{\perp} \approx J_{\perp}$.

As a next step one constructs the impurity-conduction electron scattering matrix from Eq. (B1). Introducing the impurity and the conduction electron 'rapidities', $\lambda_0 = -1$ and $\lambda_j = 0$, the s-matrix between the j 'th electron and the local impurity spin can be written as:

$$S_{0j}(\lambda_0 - \lambda_j)_{\sigma_0\sigma'_0;\sigma_j\sigma'_j}, \quad (\text{B2})$$

where — apart from some unimportant phase factors — S_{0j} can be expressed as

$$S_{0j}(\lambda) = a(\lambda)P_{\uparrow\uparrow} + b(\lambda)P_{\uparrow\downarrow} + \frac{1}{2}c(\lambda)(\sigma_0^+ \otimes \sigma_j^- + \text{h.c.}),$$

$$\frac{a(\lambda)}{c(\lambda)} = \frac{\sinh(i\mu + \lambda f)}{\sinh(i\mu)}, \quad (\text{B3})$$

$$\frac{a(\lambda)}{b(\lambda)} = \frac{\sinh(i\mu + \lambda f)}{\sinh(\lambda f)},$$

with $P_{\uparrow\uparrow}$ and $P_{\uparrow\downarrow}$ being the projection operators for parallel and opposite spins.

The parameters μ and f are connected to the bare couplings via:

$$\cos(\mu) = \frac{\cos(I_{\parallel}/2)}{\cos(I_{\perp}/2)}, \quad (\text{B4})$$

$$\text{cth}^2(f) = \frac{\sin^2(I_{\parallel}/2)}{\sin((I_{\parallel} + I_{\perp})/2)\sin((I_{\parallel} - I_{\perp})/2)}. \quad (\text{B5})$$

The electron-electron s-matrix is not determined by Eq. (B1) but is fixed by the requirement of integrability, and is simply given by $S_{ij}(\lambda_i - \lambda_j)$. With this choice the impurity-electron and electron-electron s-matrices belong to the same family of s-matrices, Eq. (B3), and satisfy the following Yang-Baxter relations:

$$S_{ij}(\alpha)S_{ik}(\alpha + \beta)S_{jk}(\beta) = S_{jk}(\beta)S_{ik}(\alpha + \beta)S_{ij}(\alpha) \quad (\text{B6})$$

insuring the integrability of the model^{13,40}. The Bethe Ansatz (BA) equations are derived using standard algebraic methods, based on Eq. (B6) by creating 'spin waves' from the completely spin-polarized state^{13,40}. The spin waves are characterized by rapidities λ_{β} ($\beta = 1, \dots, M$) and the obtained state is an eigenstate of H if these rapidities satisfy the following BA equations:

$$\prod_{\beta=1}^M \frac{\sinh(\mu(\lambda_{\alpha} - \lambda_{\beta} + i))}{\sinh(\mu(\lambda_{\alpha} - \lambda_{\beta} - i))} = -\frac{\sinh(\mu(\lambda_{\alpha} + f/\mu + i/2))}{\sinh(\mu(\lambda_{\alpha} + f/\mu - i/2))} \times \left[\frac{\sinh(\mu(\lambda_{\alpha} + i/2))}{\sinh(\mu(\lambda_{\alpha} - i/2))} \right]^{N_e}. \quad (\text{B7})$$

Thus an eigenstate of the Hamiltonian is characterized by the momenta k_j ($j = 1..N$) of the conduction electrons and the rapidities $\{\lambda_{\beta}\}$, corresponding to the charge and spin degrees of freedom, respectively. The energy of a state is determined through the periodic boundary conditions:

$$e^{ik_j L} = \prod_{\beta=1}^M \frac{\sinh(\mu(\lambda_{\beta} + i/2))}{\sinh(\mu(\lambda_{\beta} - i/2))}, \quad (\text{B8})$$

$$E = \sum_{j=1}^N k_j - hgS_z^{(\text{tot})}. \quad (\text{B9})$$

Since the λ_{β} 's ($\beta = 1, \dots, M$) are spin -1 excitations¹³ the total spin is simply $S_z^{(\text{tot})} = S^{(\text{tot})} = (N_e + 1 - 2M)/2$.

2. Thermodynamic BA equations

To derive the thermodynamic BA equations (TBA) one takes the limit $L, N \rightarrow \infty$, $N/L = D$. In this limit the rapidities λ_{α} in Eq. (B7) can be shown to organize into r -strings¹³, $\lambda_{\alpha} \rightarrow \lambda_{\beta}^{(r,v)}$ ($\beta = 1, \dots, M_{(r,v)}$), with integer ranks r and parity $v = \pm$:

$$\lambda^{(r,v)} \Leftrightarrow \lambda_{q=1,\dots,r}^{(r,v)} = \lambda^{(r,v)} + \left[\frac{r+1}{2} - q \right] + i\frac{\pi}{4\mu}(1-v). \quad (\text{B10})$$

The allowed (r, v) values must satisfy the stability condition

$$v \sin(\mu q) \sin(\mu(r-q)) > 0, \quad q = 1, \dots, [r/2], \quad (\text{B11})$$

and can be determined by expressing μ/π as an infinite (finite) fraction. For rational μ/π 's only a finite number of possible ranks and parities survive⁴¹. Specifically, for $\mu = \pi/\nu$ only the pairs

$$n = (r, v) = (1, +), (2, +), \dots, (\nu - 1, +) \text{ and } (1, -) \quad (\text{B12})$$

are allowed, which we label by $n = 1, \dots, \nu$ in what follows.

After classifying the possible strings one introduces the density of rapidities of the $n = (r, v)$ -strings, $\varrho_n(\lambda)$, and the density of 'holes', $\tilde{\varrho}_n(\lambda)$. These are connected by a linear integral equation derived from Eq. (B7) as

$$\varrho_n(\lambda) = a_n(\lambda) - \sum_{n'} \int d\lambda' K_{nn'}(\lambda - \lambda') \varrho_{n'}(\lambda'), \quad (\text{B13})$$

where the functions a_n and the Kernel $K_{nn'}$ depend only on μ . The spin part of the energy, Eq. (B9), and the entropy can be expressed as:

$$E^{(spin)} = \sum_n \int d\lambda f_n(\lambda) \varrho_n(\lambda), \quad (\text{B14})$$

$$S^{(spin)} = k_B \sum_n \int d\lambda \left[\varrho_n \ln \left(1 + \frac{\tilde{\varrho}_n}{\varrho_n} \right) + \tilde{\varrho}_n \ln \left(1 + \frac{\varrho_n}{\tilde{\varrho}_n} \right) \right].$$

Then Eqs. (19) and (22) can be derived simply by minimizing the free energy $F^{(spin)} = E^{(spin)} - TS^{(spin)}$ with respect to $\delta\varrho_n(\lambda)$ using the constraint Eq. (B13) and introducing the 'excitation energies' $\varepsilon_n(\lambda)/T \equiv \ln(\tilde{\varrho}_n/\varrho_n)$.

APPENDIX C: NUMERICAL SOLUTION THE THE THERMODYNAMIC BETHE ANSATZ EQUATIONS

In this appendix we describe in detail a new numerical procedure for solving thermodynamic Bethe Ansatz equations of the form (50) for the quantities $\xi_j, j = 1, \dots, \nu$. Such equations arise also in other contexts, for example, in the context of the anisotropic Heisenberg model⁴¹. The method we describe has the advantage that the thermodynamics is calculated without the need to take numerical derivatives of the free energy (see Sec.IVa). An implementation of this for the special case of zero field static susceptibilities has been given in³⁸ for the multichannel Kondo model and in⁴³ for the $SU(N) \times SU(f)$ Coqblin-Schrieffer model. We have gone further and have shown that other quantities, such as the entropy and in principle also the specific heat, can be calculated in the same way and for finite fields, as explicitly described in Sec.IVa. However, more importantly we show how to obtain with the same numerical procedure uniformly accurate results for thermodynamics in the presence of an *arbitrarily* large level asymmetry, ε/T , (or equivalently an arbitrarily large magnetic field, h/T , in the Kondo model). This was particularly important for obtaining the very low temperature thermodynamics

of the asymmetric two-level system in this paper. Previous techniques, for related TBA equations where the same technical difficulty arises, have either not been able to access large ε/T (h/T)³⁹ or,⁴⁴ have required solving a separate set of approximate TBA equations suitable for large ε/T (h/T). The latter requires matching the resulting thermodynamics at the boundary of the two temperature ranges.

The iterative procedure to solve the TBA equations (50) is as follows. An evenly spaced grid of 1000 points $\{\lambda_i, i = 1, \dots, 1000\}$ is used in the interval $-40 \leq \lambda \leq +40$, the functions $\xi_j(\lambda_i), j = 1, \nu$ are given initial values $\xi_j(\lambda_i) = \xi_j^{m=1}(\lambda_i)$, and are then represented by least squares cubic splines⁴². The next iteration, $\xi_j^{m=2}(\lambda_i)$, was obtained by evaluating the integrals to a relative error of less than 10^{-5} at each point for each function in turn. This procedure was repeated until the $\epsilon_j \equiv \|\xi_j^N - \xi_j^{N-1}\| / \|\xi_j^N\|, j = 1, \dots, \nu$ with $\|\xi_j\| \equiv \sqrt{\sum_i |\xi_j(\lambda_i)|^2}$ (when non-zero) reached machine precision (approximately 10^{-16}). Convergence depended on ν , with the procedure converging for a typical case after approximately 30, 44 and 61 iterations for $\alpha = (1 - 1/\nu) > 1/2$ and $\nu = 3, 4$ and 5 respectively. For fixed level asymmetry, ε , we solved the above equations at each temperature. Similarly for $\alpha = 1/\nu < 1/2$ the number of iterations required to reach convergence was typically 52, 79 and 133 for $\nu = 3, 4$ and 5 respectively.

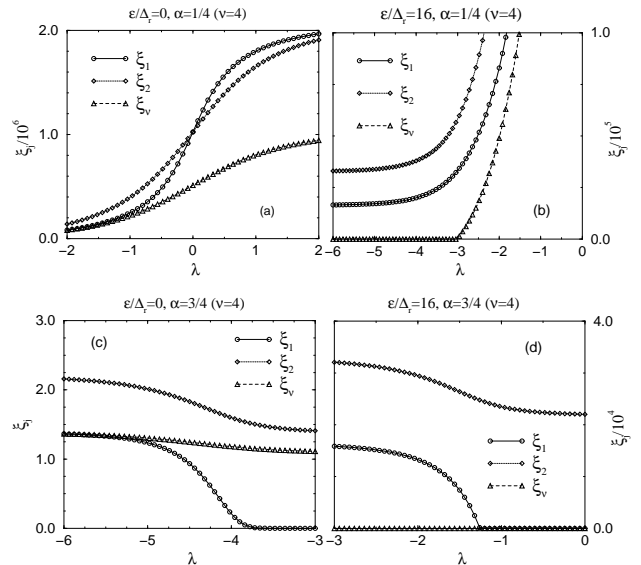


FIG. 17. Solutions to the TBA equations (50) at $\alpha T/\Delta_r = 2^{-10}$ for $\alpha = 1/4 < 1/2$ (a) and (b) (top) and $\alpha = 3/4 > 1/2$ (c) and (d) (bottom) and for zero (left) and large (right) level asymmetry. The exponential decay in ξ_1 (ξ_ν) for strong (weak) dissipation at large level asymmetries is clearly seen.

A useful check on the correctness of the solution of the TBA equations was the value of the functions ξ_j, E_j, F_j and G_j at $\lambda \rightarrow \pm\infty$. These satisfy transcendental equa-

tions which can be solved analytically or numerically¹³. We checked that our numerical solution for the above functions satisfied these boundary conditions at all temperatures and level asymmetries.

In order to indicate the difficulty one encounters in implementing the above procedure for large asymmetries and low temperatures we show some results in Fig. 17. For zero asymmetry, the functions are well behaved and have variations on scales $\lambda \sim 1$ so the interpolation scheme used above, which is crucial for carrying out the integrations accurately and ensuring the accuracy of the solution, is highly accurate. For large ε/T we see however that for $\alpha > 1/2$ ($\alpha < 1/2$) the function ξ_1 (ξ_ν) decays exponentially to a vanishingly small value above (below) a characteristic rapidity $\lambda = B$ within an interval which vanishes as $x_0 = g\varepsilon\nu/2T$ increases⁴⁵. In this case a uniform grid of points is inadequate and any interpolation will give wrong results. One could increase the density of points close to B , but a much simpler solution is not to solve explicitly for the functions ξ_1 (ξ_ν) but to solve instead for the quantities upon which they depend on (see Eq.(50)), namely $s_f(\lambda) = s * \xi_2(\lambda)$ ($s_f(\lambda) = s * \xi_{\nu-2}(\lambda)$) where $s*$ is the integral operator defined in Eq.(21). The latter functions $s_f(\lambda)$ vary on a scale of $O(1)$ and can safely be interpolated. From these one can then obtain ξ_1 (ξ_ν) via its definition (50). The characteristic energy B is determined at each iteration and used to split up the integration ranges for those integrals containing ξ_1 (ξ_ν) so that the relative error of 10^{-5} for each integration can be maintained.

The integral equations for the E_j, F_j and G_j (54–56), apart from being linear inhomogeneous integral equations as opposed to the non-linear TBA equations for the ξ_j , have an identical structure to those of the latter. As above, for large x_0 and $\alpha > 1/2$ ($\alpha < 1/2$), one has to solve explicitly not for the E_1, F_1, G_1 (E_ν, F_ν, G_ν), which vary rapidly near B as a result of the factors $(1 - e^{-\xi_1})$ ($(1 - e^{-\xi_\nu})$) appearing in the corresponding integral equations (54–56), but for the quantities $s * E_2, s * F_2, s * G_2$ ($s * E_{\nu-2}, s * F_{\nu-2}, s * G_{\nu-2}$) with splitting of the integration range for integrals involving the former. The same algorithm is therefore used as for the ξ_j . Since this turned out to be a highly stable and accurate algorithm equally applicable without changes to both sets of equation we did not consider the possibly simpler procedure of solving the linear equations for the E_j, F_j and G_j by Fourier transformation. This would involve numerically Fourier transforming the inhomogeneous terms, solving the resulting equations and then Fourier transforming the functions back to λ -space. Computationally, this would be more efficient, but may not be as accurate as the procedure we have used. In considering larger systems of coupled integral equations, $\nu \gg 1$, for which computational time is a factor, the more efficient procedure may have to be implemented.

The above technique, which resolves the problem of the exponential decay of certain functions to zero and thus allows the integrations at all points to be carried out

with uniform accuracy, gives a controlled way of solving the TBA equations. The thermodynamics is then calculated without taking any numerical derivatives. Integrating the functions ξ_1, E_1, F_1 and G_1 , weighted with $s(\lambda + f/\mu)$ as described in Sec.IV a, gives the free energy, polarization, dielectric susceptibility and entropy respectively. Fig. 18 illustrates how the above numerical difficulties were overcome for $G_1(\lambda, \varepsilon, T)$ at low temperature and large level asymmetry.

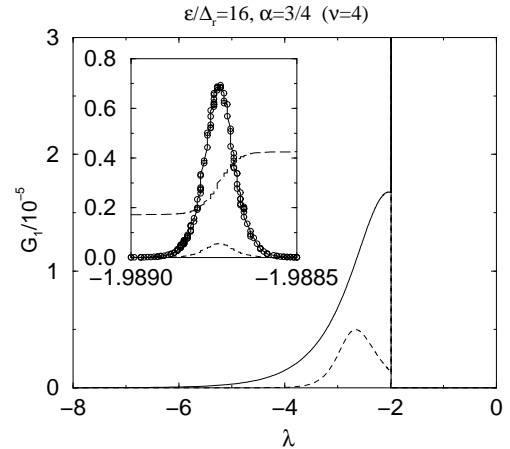


FIG. 18. $G_1(\lambda, \varepsilon, T)$ (solid line), and the integrand $s(\lambda + f/\mu)G_1(\lambda, \varepsilon, T)$ (dashed line) of the expression for the entropy in Sec.IV a. The inset shows that the spike close to $\lambda = B \approx -2$, due to the exponential decrease of ξ_1 for large level asymmetry and low temperature, is a smooth structure on a small scale which is resolved by our numerical procedure. The integrated weight $\tilde{S}(\lambda) = \int_{-40}^{\lambda} d\lambda' s(\lambda' + f/\mu)G_1(\lambda', \varepsilon, T)$ (multiplied by 40000), giving the entropy, is also shown in the inset (long dashed line). The contribution coming from the spike is seen to be approximately the same as that coming from the broad feature.

APPENDIX D: UNIVERSAL THERMODYNAMIC BETHE ANSATZ EQUATIONS FOR $\alpha < 1/2$

To derive the universal Bethe Ansatz equations one has to write Eq. (19) in a form where the cutoff ω_c , explicitly only present in the driving term Eq. (20), can safely be removed. A simple analysis of Eq. (19) shows that for $\alpha > 1/2$ in the $\lambda \rightarrow \infty$ limit all the ϵ_j 's tend to a finite value determined by T and ε (or h) except for ϵ_1 which approaches $\epsilon_1 \sim -\omega_c$ and thus diverges in the $\omega_c \rightarrow \infty$ limit. This divergence is, however, harmless, since ϵ_1 occurs only in the form $\sim \exp(\epsilon_1(\lambda))$ at the r.h.s. of Eq. (19), and therefore all the 'interaction terms' behave nicely even in the $\omega_c \rightarrow \infty$ limit.

For $\alpha < 1/2$ the situation drastically changes due to the sign change of the driving term. In this case one can easily convince himself that $\epsilon_j \sim \omega_c$ for $j = 1, \dots, \nu - 1$ while $\epsilon_\nu \sim -\omega_c$ as $\lambda \rightarrow \infty$, i.e. the interaction terms blow up as one tries to remove the cutoff. The basic

idea to obtain the universal equations is therefore to transform Eqs. (19) into a form where only $\exp(-\epsilon_j/T)$ ($j = 1, \dots, \nu - 1$) and $\exp(\epsilon_\nu/T)$ occur in the interaction terms. After a tedious calculation one finally arrives at the following equations:

$$\frac{1}{T}\tilde{g}_j = \ln(1 + e^{\epsilon_j/T}) - \sum_{l=1}^{\nu-1} B_{jl} * \ln(1 + e^{-\epsilon_l/T}) - Q_j * \ln(1 + e^{\epsilon_\nu/T}), \quad (j = 1, \dots, \nu - 1) \quad (D1)$$

$$\frac{1}{T}\tilde{g}_\nu = \epsilon_\nu/T + \sum_{l=j}^{\nu-1} Q_j * \ln(1 + e^{-\epsilon_j/T}) + K * \ln(1 + e^{\epsilon_\nu/T}), \quad (D2)$$

where the integral operators K , Q_j and B_{jl} are defined by Eqs. 6.2.27 and 6.2.6 of Ref. 13. (Note that the last one of Eqs. 6.2.27 is written in Fourier space, and that the $a_j(\lambda)$'s occurring in the definition of A_{jk} are the functions given by the *first line* in Eq. 6.2.6 for all indices, j . Furthermore, in Eq. 6.2.6 the last δ_{jk} term must be dropped in the definition of A_{jk} .)

The driving terms, \tilde{g}_j in the equations above are defined as

$$\tilde{g}_\nu = -\tilde{g}_{\nu-1} = -\omega_c \text{artan} e^{\pi\lambda/(\nu-1)}, \quad (D3)$$

$$\tilde{g}_{j=1, \dots, \nu-2} = \omega_c \left[\frac{\pi}{2} + \text{artan} \left\{ \frac{\sinh(\frac{\pi\lambda}{\nu-1})}{\sin(\frac{\pi j}{2(\nu-1)})} \right\} \right], \quad (D4)$$

where we corrected a factor of two with respect to Eqs. 6.2.28 of Ref. 13. Finally, approximating \tilde{g}_j as $\tilde{g}_j = c_j \exp\{\pi\lambda/(\nu-1)\}$ and defining the dimensionless functions $\varphi_j(\lambda) \equiv \epsilon_j(\lambda + \frac{\nu-1}{\pi} \ln \frac{T}{\omega_c})/T$ one arrives at the following cutoff-independent universal equations:

$$d_j = \ln(1 + e^{\varphi_j}) - \sum_{l=1}^{\nu-1} B_{jl} * \ln(1 + e^{-\varphi_l}) - Q_j * \ln(1 + e^{\varphi_\nu}), \quad (j = 1, \dots, \nu - 1) \quad (D5)$$

$$d_\nu = \varphi_\nu + \sum_{l=j}^{\nu-1} Q_j * \ln(1 + e^{-\varphi_j}) + K * \ln(1 + e^{\varphi_\nu}), \quad (D6)$$

where the 'universal' driving terms are defined as

$$d_{j=1, \dots, \nu-2}(\lambda) = 2 \left(\sin \frac{\pi j}{2(\nu-1)} \right) \exp \left(\frac{\lambda\pi}{\nu-1} \right),$$

$$d_\nu = -d_{\nu-1} = -\exp \left(\frac{\lambda\pi}{\nu-1} \right).$$

These universal equations, apart from some sign changes, coincide with Eqs. 6.2.29 of Ref 13. Finally, after some manipulations the impurity contribution to the free energy can be written as

$$F^{(i)} = -\frac{T}{\pi\omega_c} \sum_{j=1}^{\nu} \int_{-\infty}^{\infty} v_j \frac{d\tilde{g}_j(\lambda + \frac{\nu-1}{\pi} \ln \frac{T}{T_K})}{d\lambda} \ln(1 + e^{-v_j\varphi_j(\lambda)}) d\lambda, \quad (D7)$$

where $v_j = +$ for $j = 1, \dots, \nu - 1$ and $v_\nu = -$. The Kondo temperature T_K (renormalized tunneling amplitude) emerges naturally in course of the calculations, and is given by

$$T_K(\alpha < 1/2) = 2De^{-\nu f/(\nu-1)} \equiv \Delta_r/\alpha, \quad (D8)$$

which is identical with Eq. (27).

We have checked that the solution of the above thermodynamic Bethe Ansatz equations gives identical results for the specific heat and static susceptibility as the much simpler equations from which they are derived. Fig. 19 shows a comparison for the specific heat calculated using the two sets of equations.

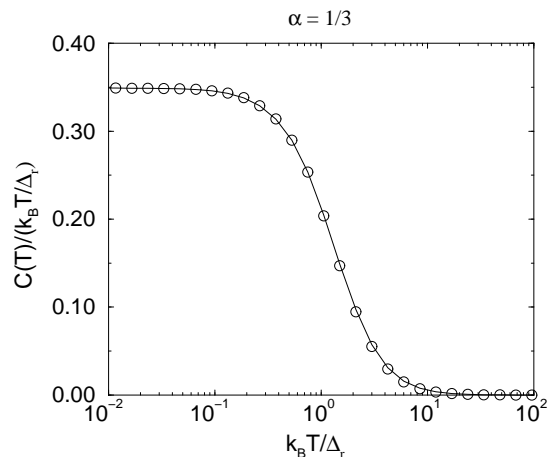


FIG. 19. Specific heats, $C(T)/T$, for the symmetric two-state system ($\varepsilon = 0$) at $\alpha = 1/3$ from (a) the universal form of the TBA equations (circles) and (b) the original untransformed TBA equations (solid line).

[†] e-mail: tac@physik.uni-augsburg.de

[‡] e-mail: zarand@phy.bme.hu

¹ Present address.

² Present address.

¹ A. J. Leggett, in *Percolation, Localization and Superconductivity*, Vol. 109 of *NATO Advanced Study Institute, Series B: Physics*, edited by M. Goldman and S. A. Wolf (Plenum, New York, 1984).

² R. Konik and A. LeClair, *Phys. Rev. B* **58**, 1872 (1998); A. Leclair, F. Lesage, S. Lukyanov and H. Saleur, *Phys. Lett. A* **235**, 203 (1997).

- ³ K.S. Ralls and R. A. Buhrman, Phys. Rev. Lett. **60**, 2434 (1988); B. Golding, N. Zimmerman, and S. Coppersmith, Phys. Rev. Lett. **68**, 998 (1992).
- ⁴ For a review see A. J. Leggett, S. Chakravarty, A. T. Dorsey, M. P. A. Fisher, A. Garg and W. Zwerger, Rev. Mod. Phys. **59**,1 (1987); **67**, 725 (1995).
- ⁵ U. Weiss, in *Series in Modern Condensed Matter Physics*, edited by I.E.Dzyaloshinskii, S. O. Lundqvist and Yu Lu (World Scientific, Singapore, 1999), Vol. 2, 2nd edition.
- ⁶ A. O. Caldeira and A. J. Leggett, Ann. Phys. (N.Y.) **149**, 374 (1984); **153**, 445(E), (1984).
- ⁷ For a review see^{4,5}. For some recent work see²²⁻²⁶; S. K. Kehrein and A. Mielke, Annalen der Physik, **6**, 90 (1996); S. P. Strong, Phys. Rev. E**55**, 6636 (1997); G. Lang, E. Paladino and U. Weiss, Europhys. Lett. **43**, 117 (1998).
- ⁸ We define “coherence” to mean the presence of oscillatory contributions to real time dynamical quantities, such as $\Im\langle\sigma_z(t)\sigma_z(0)\rangle$ and $\Re\langle\sigma_z(t)\sigma_z(0)\rangle$. This implies that the system exhibits phase coherence in time.
- ⁹ Certain correlations, such as $\Re\langle\sigma_z(t)\sigma_z(0)\rangle$, have long time $1/t^2$ tails at $T = 0$ as their leading contribution. The exponential decay then refers to the oscillatory contribution which is a subleading contribution
- ¹⁰ A. J. Bray and M. A. Moore, Phys. Rev Lett. **49**, 1545 (1982); S. Chakravarty, Phys. Rev Lett. **50**, 1811 (1982).
- ¹¹ A. Zawadowski, Phys. Rev. Lett. **45**, 211 (1980); K. Vladar and A. Zawadowski, Phys. Rev. B **28**, (a) 1564; (b) 1582; (c) 1596 (1983).
- ¹² A. L. Moustakas and D. S. Fisher, Phys. Rev. B **51**, 6908 (1995).
- ¹³ A. M. Tselvelik and P. B. Wiegmann, Adv. Phys. **32**, 453 (1983).
- ¹⁴ A. C. Hewson, *The Kondo problem to heavy fermions*, Cambridge University Press, (1993).
- ¹⁵ G. Grüner and A. Zawadowski, Rep. Prog. Phys. **37** 1497 (1974).
- ¹⁶ G. Toulouse, Compt. Rend. Acad. Sci. Paris **268**, 1200 (1969).
- ¹⁷ T. A. Costi, Phys. Rev. Lett. **80**, 1038 (1998).
- ¹⁸ R. Görlich and U. Weiss, Phys. Rev. B**38**, 5245 (1988).
- ¹⁹ This difficulty is due to the fact that the local S_z in the AKM is not conserved as opposed to total z-component of the spin. A discussion where this problem arises for similar quantities can be found in T. A. Costi, Phys. Rev. B **55**, 3003 (1997).
- ²⁰ By tunneling regime we mean the regime where there is a finite renormalized tunneling amplitude Δ_r . In the limit $\Delta/\omega_c \rightarrow 0$ this region is $0 < \alpha \leq 1$. For finite Δ/ω_c it depends also on Δ/ω_c as discussed in Sec.IIc. The tunneling regime consists of two qualitatively different regions, distinguished by the presence (for $0 < \alpha < 1/2$) or absence (for $1/2 < \alpha < 1$) of tunneling oscillations in *time dependent* quantities.
- ²¹ P. Schlottmann, Phys. Rev. B**25**, 4815 (1982); F. Guinea, V. Hakim and A. Muramatsu, Phys. Rev. B**32** 4410, (1985).
- ²² S. Chakravarty and J. Rudnick, Phys. Rev. Lett. **75**, 501 (1995).
- ²³ T. A. Costi and C. Kieffer, Phys. Rev. Lett. **76**, 1683 (1996).
- ²⁴ F. Lesage, H. Saleur and S. Skorik, Phys. Rev. Lett. **76**, 3388 (1996).
- ²⁵ K. Völker, Phys. Rev. B **58**, 1862, (1998).
- ²⁶ F. Lesage and H. Saleur, Phys. Rev. Lett. **80**, 4370,(1998).
- ²⁷ K. G. Wilson, Rev. Mod. Phys. **47**, 773 (1975).
- ²⁸ H. B. Krishnamurthy, J. W. Wilkins & K. G. Wilson, Phys. Rev. B**21**, 1003 (1980).
- ²⁹ G. Kotliar and Q. Si, Phys. Rev. B**53**, 12373 (1996).
- ³⁰ P. W. Anderson, G. Yuval and D. R. Hamann, Phys. Rev. B**1** 4464, (1970).
- ³¹ Note, however, that in region $B \Delta/\omega_c$ can be irrelevant to start with for $\alpha_0 > 1$, but will eventually become relevant once α decreases to $\alpha < 1$. This does not happen in regions A and C .
- ³² The appearance of the factor of α relating the two scales Δ_r and T_K stems from the introduction of electron-electron interactions into the AKM to ensure integrability within the Bethe Ansatz (without such interactions we could simply write $\Delta_r = T_K$). This results in susceptibilities being renormalized by a factor $1/\alpha$ within the Bethe Ansatz calculations (see Sec. IIIB3 for details), so in order to relate the scales of the AKM and the Ohmic two-state system from the $T = 0$ susceptibility of the Bethe Ansatz calculation one needs to include this factor.
- ³³ P. Nozières, J. Low Temp. Phys. **17**, 13 (1975).
- ³⁴ K. Yoshida and K. Yamada, Prog. Theor. Phys. **46**, 244 (1970); *ibid.* **53**, 1286 (1975).
- ³⁵ We emphasize the distinction we are making between the susceptibility of the AKM and the susceptibility of the AKM calculated from the BA which involves modifications to the model in order to make it integrable. The distinction, as shown below, is important.
- ³⁶ P. B. Viggmann and A. M. Finkel’shtein, Sov. Phys. JETP **48**,102 (1978)
- ³⁷ M. Sasseti and U. Weiss, Phys. Rev. Lett. **65**, 2262 (1990).
- ³⁸ H. U. Desgranges, J. Phys. C. **18**, 5481 (1985).
- ³⁹ V. T. Rajan, J. H. Lowenstein and N. Andrei, Phys. Rev. Lett. **49**, 497 (1982)
- ⁴⁰ N. Andrei, in *Series on Modern Condensed Matter Physics*, Lecture Notes of ICTP Summer Course, September 1992, edited by S. Lundquist, G. Morandi and Yu Lu (World Scientific, Singapore, 1995), Vol. 6, 458-551.
- ⁴¹ M. Takahashi and M. Suzuki, Prog. Theor. Phys. **48**, 2187 (1972); *ibid.* **50**, 1519 (1973); *ibid.* **50**, 1519 (1973).
- ⁴² We used those in the Numerical Algorithms Group (NAG) library.
- ⁴³ A. Jerez, N. Andrei and G. Zaránd, Phys. Rev. B **58**, 3814 (1998).
- ⁴⁴ P. D. Sacramento, Phys. Rev. B**43**, 13294 (1991).
- ⁴⁵ The reason for the exponential decay of ξ_1 (ξ_ν) for $\alpha > 1/2$ ($\alpha < 1/2$) is clear from the form of ξ_1 (ξ_ν) and the values which the functions ξ_j take at the boundaries $\lambda \rightarrow \pm\infty$. For definiteness consider $\alpha > 1/2$, then $\xi_1 = \ln[1 + \exp(D(\lambda) + s * \xi_2 + \delta_{1,\nu-2} s * \xi_3)]$. It can be shown that the ξ_j are monotonically decreasing and for $\varepsilon/T \gg 1$ take on values at $\pm\infty$ of order ε/T . Due to the negative driving term in ξ_1 the sign of the term in the exponential will change at some $\lambda = \lambda_0$ from a very large positive value to a very large negative value thereby giving rise to the exponential decay in ξ_1 . A similar reason holds for the function ξ_ν in the case

- $\alpha < 1/2$ for $\varepsilon/T \gg 1$ (the large terms in the exponential now being x_0 and $s * \xi_{\nu-2}$).
- ⁴⁶ D. Vollhardt, Phys. Rev. Lett. **78**, 1307 (1997).
- ⁴⁷ The appearance of a well defined oscillatory mode, in the sense we have described, should be distinguished with the appearance of tunneling oscillations or “coherence” which happens at $\alpha = 1/2^8$.
- ⁴⁸ H. Wipf and K. Neumaier, Phys. Rev. Lett. **52**, 1308 (1984).
- ⁴⁹ S. Katayama, S. Maekawa, and H. Fukuyama, J. Phys. Soc. Jpn. **50**, 694 (1987).
- ⁵⁰ Jan von Delft and H. Schoeller, Annalen der Physik **7**, 225 (1998).
- ⁵¹ For a review see V. J. Emery and S. A. Kivelson, in *Fundamental Problems in Statistical Mechanics VIII*, edited by H. van Beijeren and M. H. Ernst, pp. 1-24, Elsevier, Amsterdam, (1994).
- ⁵² A. Schiller and K. Ingersent, Phys. Rev. **B51**, 4676 (1995).
- ⁵³ X. Wang, Mod. Phys. Lett. **B12**, 667 (1998).
- ⁵⁴ T. Brugger, T. Schreiner, G. Roth, P. Adelman, and G. Czjzek, Phys. Rev. Lett. **71**, 2481 (1993).
- ⁵⁵ P. Fulde and V. Zevin, Europhys. Lett. **24**, 791 (1993); P. Fulde, V. Zevin and G. Zwicknagel, Z. Phys. **B92**, 133 (1993).
- ⁵⁶ Jan von Delft, G. Zaránd, and M. Fabrizio, Phys. Rev. Lett. **81**, 196 (1998); G. Zaránd, and Jan von Delft, Phys. Rev. B.
- ⁵⁷ A. Muramatsu and F. Guinea, Phys. Rev. Lett. **57**, 2337 (1986).